Centrifugal projections to the main olfactory bulb revealed by trans-synaptic retrograde tracing in mice

Nanette Schneider, Sylvie Chaudy, Alberto L. Epstein, Cécile Viollet, Alexandre Benani, Luc Pénicaud, Xavier Grosmaître, Frédérique Datiche, Jean Gascuel

Title: Centrifugal projections to the main olfactory bulb revealed by trans-synaptic retrograde tracing in mice

Abbreviated title: Polysynaptic afferents to the main olfactory bulb

Nanette Y Schneider, [1] Sylvie Chaudy, [1] Alberto L Epstein, [2] Cécile Viollet, [3] Alexandre Benani[1], Luc Pénicaud, [1,4] Xavier Grosmaître, [1] Frédérique Datiche, [1*] Jean Gascuel [1*]

[1] 1 Centre des Sciences du Goût et de l'Alimentation (CSGA), UMR 6265 CNRS / 1324 INRA / Université de Bourgogne Franche-Comté, Dijon, France.
[2] UMR 1179 INSERM-UVSQ—End-icap, Université de Versailles-Saint Quentin en Yvelines, France;
[3] INSERM U1266, IPNP, Institut de Psychiatrie et Neuroscience de Paris, Paris, France
[4] Present address : Stromalab, CNRS ERL 5311-Université Paul Sabatier, Toulouse, France

***Corresponding authors:** Jean Gascuel, CSGA, CNRS UMR 6265 Centre des Sciences du Goût et de l'Alimentation, 21000 Dijon, France. Email: jean.gascuel@u-bourgogne.fr, Frédérique Datiche, CSGA, CNRS UMR 6265 Centre des Sciences du Goût et de l'Alimentation, 21000 Dijon, France. Email: frederique.datiche@u-bourgogne.fr

Acknolwledgments: We are grateful to the professor Lynn Enquist for having kindly provided the viruses used in this study. We would like to thank Pierre Yves Risold for helpful discussion relating to this work, and the generous gift of antibodies. We thank Anne Lefranc for their help for animal care. This work was supported by grants from the Conseil Régional Bourgogne, Franche-Comté (PARI grant), the FEDER (European Funding for Regional Economical Development), and INRA AlimH department.

Data Availability Statement : The data that support the findings of this study are available from the corresponding author upon reasonable request.

This article has been accepted for publication and undergone full peer review but has not been through the copyediting, typesetting, pagination and proofreading process which may lead to differences between this version and the Version of Record. Please cite this article as doi: 10.1002/cne.24846

Abbreviations :

3V	3rd ventricle
4V	4th ventricle
Acb	accumbens nucleus
ACo	anterior cortical amygdaloid area
AHi	amygdalohippocampal area
AHiPM	amygdalohippocampal area, posteromedial part
AID	agranular insular cortex, dorsal part
AIP	agranular insular cortex, posterior part
AIV	agranular insular cortex, ventral part
AON	anterior olfactory nucleus
aPir	piriform cortex anterior part
Arc	arcuate hypothalamic nucleus
Au1	primary auditory cortex
AuD	secondary auditory cortex, dorsal area
AuV	secondary auditory cortex, ventral area
BLA	basolateral amygdaloid nucleus, anterior part
BLP	basolateral amygdaloid nucleus, posterior part
BMA	basomedial amygdaloid nucleus, anterior part
BMP	basomedial amygdaloid nucleus, posterior part
CA1	field CA1 of the hippocampus
CA2	field CA2 of the hippocampus
CA3	field CA3 of the hippocampus
Ce	central amygdaloid nucleus
cg	cingulum
Cg1	cingulate cortex, area 1

This article is protected by copyright. All rights reserved.

Cg2	cingulate cortex, area 2
CI	Island of Calleja
Cl	claustrum
cp	cerebral peduncle
CxA	cortex-amygdala transition zone
DG	dentate gyrus
DI	dysgranular insular cortex
DLEnt	dorsolateral entorhinal cortex
DM	dorsomedial hypothalamic nucleus
DMPAG	dorsomedial periaqueductal gray
DR	dorsal raphe nucleus
DRD	dorsal raphe nucleus, dorsal part
DRL	dorsal raphe nucleus, lateral part
DRV	dorsal raphe nucleus, ventral part
DTT	dorsal tenia tecta
Ect	ectorhinal cortex
En	endopiriform claustrum
Fr3	frontal cortex, area 3
Gi	gigantocellular reticular nucleus
GI	granular insular cortex
Gr	granule cell layer of the olfactory bulb
HDB	nucleus of the horizontal limb of the diagonal band
Hippo	Hippocampus
IL	infralimbic cortex
IPR	interpeduncular nucleus, rostral subnucleus
IRt	intermediate reticular nucleus

This article is protected by copyright. All rights reserved.

La	lateral amygdaloid nucleus
LC	locus coeruleus
LDT	laterodorsal tegmental nucleus
LDTgV	laterodorsal tegmental nucleus, ventral part
LH	lateral hypothalamic area
LHb	lateral habenular nucleus
LO	lateral orbital cortex
LOT	nucleus of the lateral olfactory tract
LPAG	lateral periaqueductal gray
LPO	lateral preoptic area
LRt	lateral reticular nucleus
LSD	lateral septal nucleus, dorsal part
LSI	lateral septal nucleus, intermediate part
LSO	lateral superior olive
LSV	lateral septal nucleus, ventral part
M1	primary motor cortex
M2	secondary motor cortex
MCPO	magnocellular preoptic nucleus
MD	mediodorsal thalamic nucleus
Me	medial amygdaloid nucleus
MEnt	medial entorhinal cortex
mlf	medial longitudinal fasciculus
MnR	median raphe nucleus
MO	Medial orbital cortex
MOB	Main olfactory Bulb
MS	medial septal nucleus

This article is protected by copyright. All rights reserved.

MTu	medial tuberal nucleus
Pa	paraventricular hypothalamic nucleus
PAG	periaqueductal gray
PBP	parabrachial pigmented nucleus of the VTA
PH	posterior hypothalamic nucleus
Pir	piriform cortex
PLCo	posterolateral cortical amygdaloid area
PMCo	posteromedial cortical amygdaloid area
PnO	pontine reticular nucleus, oral part
PRh	perirhinal cortex
PrL	prelimbic cortex
PSTh	parasubthalamic nucleus
PV	paraventricular thalamic nucleus
Re	reuniens thalamic nucleus
Rh	rhomboid thalamic nucleus
RSD	retrosplenial dysgranular cortex
RVL	rostroventrolateral reticular nucleus
S	subiculum
S1	primary somatosensory cortex
S1BF	primary somatosensory cortex, barrel field
S2	secondary somatosensory cortex
S2	secondary somatosensory cortex
SCh	suprachiasmatic nucleus
SNC	substantia nigra, compact part
SNR	substantia nigra, reticular part
SO	supraoptic nucleus

This article is protected by copyright. All rights reserved.

Sol	solitary nucleus
Sp5I	spinal trigeminal nucleus, interpolar part
STh	subthalamic nucleus
TeA	temporal association cortex
Tu	olfactory tubercle
V1	primary visual cortex
V2	secondary visual cortex
VDB	nucleus of the vertical limb of the diagonal band
VMH	ventromedial hypothalamic nucleus
VO	ventral orbital cortex
VP	ventral pallidum
VTA	ventral tegmental area
VTg	ventral tegmental nucleus
VTM	ventral tuberomammillary nucleus
VTT	ventral tenia tecta
Xi	xiphoid thalamic nucleus
ZI	zona incerta

This article is protected by copyright. All rights reserved.

ABSTRACT

A wide range of evidence indicates that olfactory perception is strongly involved in food intake. However, the polysynaptic circuitry linking the brain areas involved in feeding behaviour to the olfactory regions is not well-known. The aim of this paper was to examine such circuits. Thus, we described, using hodological tools such as trans-synaptic viruses (PRV152) transported in a retrograde manner, the long-distance indirect projections (2-3 synapses) onto the main olfactory bulb (MOB). The b-subunit of the cholera toxin (CTb) which is a monosynaptic retrograde tracer was used as a control to be able to differentiate between direct and indirect projections. Our tracing experiments showed that the arcuate nucleus of the hypothalamus, as a major site for regulation of food intake, sends only very indirect projections onto the MOB. Indirect projections to MOB also originate from the solitary nucleus which is involved in energy homeostasis. Other indirect projections have been evidenced in areas of the reward circuit such as VTA and accumbens nucleus. In contrast, direct projections to the MOB arise from MCH- and Orx neurons in the lateral hypothalamus. Functional significances of these projections are discussed in relation to the role of food odors in feeding and reward-related behavior.

Keywords: pseudorabies virus, choleratoxin b subunit, odor processing, feeding behavior, reward.

RRID:AB_300798; RRID:AB_726859; RRID:AB_956454; RRID:AB_2269954; RRID:AB_2302603; RRID:AB_2636803; RRID:AB_2650474; RRID:AB_2534069; RRID:AB_297689; RRID:AB_142754; RRID:AB_2534091; RRID:AB_141521

This article is protected by copyright. All rights reserved.

1. INTRODUCTION

A wide range of evidence indicates that several closely linked systems control feeding behavior. Besides energy intake, eating involves a sensory experience. It is established that odors play a key role before, during and after the meal. Thus, olfaction is at the forefront of the sensory systems involved in feeding behavior. Two well-known phenomena illustrate the modulation of the perception of food odors. Firstly, sensory-specific satiety (Rolls, Rolls, Rowe, & Sweeney, 1981) represents the progressive decrease in pleasantness of a given food odor while this food is eaten to satiety during a meal. Meanwhile, pleasantness of other food odors does not change. Secondly, olfactory allesthesia allows post-consumption appetite to be suppressed, and participates to meal termination (Duclaux, Feisthauer, & Cabanac, 1973). Indeed, the pleasantness of a food odor is high when the subject is hungry, and decreases when the subject is satiated. Humoral mechanisms are clearly involved in these phenomena (as reviewed by Palouzier-Paulignan et al., 2012). However, some authors (Pager, Giachetti, Holley, & Le Magnen, 1972), suggested that neuronal circuits may also play a part in the control of olfactory perception by activating centrifugal modulatory pathways (Guevara-Aguilar & Aguilar-Baturoni, 1978), for instance from the hypothalamus - an area of the brain involved in energy balance control.

Normal feeding behavior retains a stable body weight, which is based on an equilibrium between systems processing both metabolic and sensory signals. Considering the key role that olfaction plays in both meal initiation and termination, it is especially important to know the central brain pathways that modulate odor perception. As of date, there is no data on polysynaptic pathways putatively involved in centrifugal modulation of the main olfactory bulb (MOB): the first central step of the olfactory system. Whether these neuronal circuits originate from the hypothalamic or the reward system is still not understood well. Answering these questions requires the study of the long-range circuits using transsynaptic neuronal tracing. The afferent connectivity to the MOB has been investigated using monosynaptic tracers (Hintiryan et al., 2012; Boyd, Sturgill, Poo, & Isaacson, 2012; Miyamichi et al., 2011) and recently by using polysynaptic tracer (Wen et al., 2019). However, the present study aimed to describe indirect projection to the CGL of the MOB arising from a wide range of areas, in particular

This article is protected by copyright. All rights reserved.

those participating in feeding behavior. Here, we used a pseudorabies virus (PRV 152), a replication-competent but attenuated neurotropic virus, to trace the transsynaptic projections onto the MOB. The PRV 152 is able to infect neurons and generate progeny which cross synapses in the retrograde direction within functional circuits (Boldogköi et al., 2004 ; Enquist & Card, 2003). Our goal was to draw a detailed map of the secondary projections onto the MOB. Even though direct projections onto the MOB have been studied extensively, we used CTb as a monosynaptic tracer as a means of controlling direct and indirect projection differentiation. Using immunohistochemical double-labeling, we characterized the chemical nature of some of the projecting neurons. We concentrated on monoamines involved in arousal, and on neuropeptides involved in food intake. The functional significance of the centrifugal projections onto the MOB is discussed in relation to the role of odor perception changes in the way feeding behavior is regulated.

2. MATERIALS AND METHODS

2.1Animals

C57 BL/6J mice used for the study were bred in our local animal facilities (CSGA, CNRS-INRA-Université de Bourgogne). Mice were housed in temperature controlled conditions (21–23°C) and a light/dark rhythm of 12:12 hours, with *ad libitum* access to food and water (AO4 standard maintenance diet; SAFE, Épinay-sur-Orge, France). Care and handling of animals were performed according to the Guidelines of the European Union Council 2010/63/UE and validated by the ethical committee n°APAFIS#5673-2016112331517261 6v1

2.2. Tracers

Polysynaptic tracing was performed using pseudorabies virus (PRV), a member of the alpha herpes virus family, which has an extensive host range except in higher primates. The virus used in this study (PRV 152) is isogenic with the attenuated Bartha strain of PRV, which induces reduced symptoms in experimental animals. PRV 152 contains the CMV-EGFP reporter gene cassette inserted into the gG locus of the viral genome. The CMV promoter drives

This article is protected by copyright. All rights reserved.

expression of the EGFP gene allowing the viral infection to be traced, and hereby the circuits. PRV 152 was generously provided by Prof Lynn Enquist. The virus was produced and titrated on PK15 cells as already described (Smith & Enquist, 2000). PRV 152 solution titer was 3.10^9 PFU/ml of culture media. To check localization of the injection site, we co-injected 1µl of a fluorospheres solution (1:100 in 0.9% NaCl), mixed with 10µl of PRV 152 solution. Fluorospheres were 1µm diameter, blue 365-415; molecular probes F8814.

Monosynaptic tracing was performed by injecting the β subunit of the cholera toxin (CTb, Sigma C9903) prepared as follows: 3µl of 5% CTb solution and 1µl of a fluorospheres solution (1:100 in 0.9% NaCl) were diluted in 10µl PBS.

2.3. Surgery and stereotactic injection procedure

Mice were injected with 0.1mg/kg buprenorphine (i.p) 20 min prior to experiments to reduce pain. Animals were then anesthetized using gaseous isoflurane at 2.5% (induction) and maintained at 1.5% during surgery. Mice were mounted on the stereotactic device. The drill was positioned above the medial part of the MOB (Bregma 4.28mm ; Lateral axis 1mm) and a hole was drilled in the skull after incision of the skin. Then a nanofil (34 gauge blunt needle, WPI NF34BL) was inserted 2.5mm deep in order to inject into the granular cell layer (GCL) of the MOB. Either 100nl of CTb or 100nl of a solution containing the PRV 152 (3.10^9 PFU/ml) and fluorospheres were injected at the speed of 20nl/min. After injection, the nanofil was left in place for 15 min in order to allow for all the 100nl to come out of the needle. Then, mice were allowed to recover after the injection of 300µl of 0.9 % NaCl, and another injection of buprenorphine.

We focused our injections on the granular cell layer which has been described as a main target of centrifugal afferents (Matsutani & Yamamoto, 2008). The injected volume and viral particle concentration were adjusted to make sure that viral tracing did not contaminate neighboring brain regions, such as the accessory olfactory bulb and the anterior olfactory nucleus. As a result, fluorospheres were reproducibly located in the granular layer of the MOB (Fig 1). The diffusion of both PRV (Fig 1 a-c1) and CTb (Fig 1 d-f1) was very limited. In a very few cases, microspheres were observed along the scar of the nanofil. Therefore, viral contamination of

This article is protected by copyright. All rights reserved.

other layers of the MOB is a possibility that would not affect in anyway the aim of this study which is to examine projections onto the MOB considered as a whole.

CTb is known to not cross synapses and to label neurons in a retrograde manner. In contrast, the PRV 152 crosses synapses, and has been used to trace the chain of indirect projections to the MOB in a retrograde manner. Thus, the comparison between CTb maps and PRV 152 maps has enabled direct projections to be distinguished from indirect ones.

2.4. Temporal consideration of viral polysynaptic tracing

Due to the fact that the replication and transmission of viruses are time-dependent, the pattern of labeled neurons changes over the course of the survival period, as cells progress through stages of infection. Here, we sacrificed mice at either 1,2,3,4 days post-injection to examine the kinetics of polysynaptic tracing. The best time points for labeling the chain of connected neurons projecting to the MOB appeared to be days 2 and 3 after injection. On day 4, we noted that nearly all the brain was infected, and the earliest infected neurons started to become apoptotic. Thus, day 4 post injection mice were not useful in this study.

2.5. Temporal consideration of monosynaptic CTb tracing

As CTb migration time is different, mice were sacrificed 14 days after the CTb injection in order to ensure complete migration of the tracer. Following this, mice were deeply anaesthetized with equithesine (4.73 ml/kg) and then intracardially perfused with 4% paraformaldehyde in phosphate buffer (PB). Brains were dissected and post-fixed for 2 hr in the same fixative.

2.6. Brain sections

Coronal brain sections of 50µm thickness, from 7.72 mm to -4.32 mm according to the interaural line (Franklin & Paxinos, 2007), were obtained using a vibroslicer (Leica). Serial sections were stored 6 by 6 in wells of a 24-well plate. Sections were cryoprotected (ethylene glycol 30%, glycerol 30%, Tris HCl 0.2M, Tris Base 0.04M, NaCl 0.15M in distilled water) before being frozen at -20°C.

This article is protected by copyright. All rights reserved.

2.7. Immunohistochemical procedures

Table 1 summarizes the different concentrations and incubation times of the antibodies and serum used in the present study. In brief, basic steps of the immunohistological procedures were the following: First of all, sections were blocked in serum diluted in PBST for 2hr, and further incubated in primary antibody for 48hr at 4°C. Secondly, sections were incubated in secondary antibody at 4°C for 48hr. Between these steps, sections were washed three times for 2 hr. Lastly, sections were incubated in Hoechst solution to counterstain nuclei and mounted with Mowiol medium.

2.8. Data analysis

Each section was photographed using a Zeiss Imager M2 microscope at 10x magnification in mosaic mode, allowing the complete 2D reconstruction of the whole section using Zeiss Axiovision software. The resulting mosaic images were analyzed, and the neuroanatomical location of the labeled cells was reported on selected levels of the Franklin and Paxinos (2007) mouse brain atlas. Figure 2 results of a compilation of 4 animals for CTb, 4 for 2 days PRV and 4 for 3 days PRV.

3. RESULTS

3.1. Direct projections to the MOB

Direct projections onto the MOB have been described extensively in the literature. In this paper, CTb (a monosynaptic tracer) was used mainly as a control to differentiate direct and indirect projections (revealed by trans-synaptic PRV 152). Our main findings are summarized below.

The olfactory tubercle excepted (Fig 2. b1), all the olfactory regions receiving bulbar projections via the lateral olfactory tract showed retrogradely labeled cells (Fig 2; Fig 3a): for instance the NOA, piriform cortex, TT, superficial amygdala nuclei, NLOT, lateral entorhinal cortex. We also confirmed that the MOB receives projections arising from basal forebrain (HDB, MCPO), raphe nuclei and locus coeruleus. In the raphe nuclei we showed double stained

This article is protected by copyright. All rights reserved.

neurons for CTb and 5 HT but some cells were only positive for CTb. We observed that in the locus coeruleus, a moderate number of CTb labeled neurons were positive for TH (not shown).

In addition, we observed projections which were not previously described. A few CTb cells appeared in the ventral pallidum (Fig 2, b1; Fig 3 a-a1). A few number of cells were also observed in the ventral tuberomamillary hypothalamic nucleus (VTM) (Fig 2, g1; Fig 3 b-b1).

The LH exhibited some CTb labeled cells. The LH is known to contain neuropeptides such as Melanin-concentrating-hormone (MCH) and orexin (Orx) neurons which play a role in energy accumulation and expenditure (Gonzales et al., 2016). Therefore, we performed double immunostainings to compare CTb labeled cells with MCH- or Orx- expressing populations. We observed a co-localization of CTb with either MCH (Fig 4a) or Orx (Fig 4b) in a moderate number of retrogradely labeled neurons.

Calcium-binding proteins (parvalbumin, calretinin, calbindin) are useful to characterize lateral hypothalamus nuclei (Celio, 1990). We also performed double-immunocytochemistry to stain these proteins. Here, no colocalization of CTb with calbindin, parvalbumin and calretinin was found (not shown).

In the hippocampal formation only the CA1 (Fig 2, i1) subdivision of the ventral hippocampus was moderately stained.

The VTA showed a low number of CTb labeled neurons while no retrogradely labeled neuron was observed in the substantia nigra. In the VTA the CTb labeled cells were TH positive (Fig 5).

3.2. Indirect projections to the MOB

All the brain areas showing cells stained retrogradely for PRV152, but not for CTb, can be considered as being indirectly connected to the MOB. As illustrated in figure 2, a wide range of regions along the whole rostro-caudal extent of the brain showed PRV labeled cells on the 2^{nd} and 3^{rd} days after bulbar injection. Nevertheless, in the text we report only areas of interest regarding the top-down olfactory modulation of feeding behavior.

This article is protected by copyright. All rights reserved.

On the 2nd day following PRV injection, analysis of the ventral striatum indicated a moderate staining in the olfactory tubercle and in the nucleus accumbens (Acb) (Fig 2, c2).

In the neocortical regions, the medial- orbital (MO) and orbito-frontal (LO/VO) cortical regions contained a noticeable number of PRV-labeled cells (Fig 2, a2) two days after PRV injection. We also observed labeled cells in the ventral (AIV) and dorsal part (AID) of the agranular insular cortex (Fig 2, b2, c2). Caudally, we found the heaviest labelling in the dysgranular (DI), posterior part of the agranular (AIP) and granular part (GI) of the insular cortex (Fig 2, d2, e2).

In the deep amygdala, both the basolateral (BLA) and basomedial (BMA) nuclei showed a conspicuous number of labeled neurons on the 3rd day (Fig 2, e3, f3). Conversely, the lateral (La) and medial (Me) amygdala nuclei (Fig 2, e3, f3) exhibited a substantial number of PRV cells only on the 3rd post-injection day. Among the amygdala nuclei, the central nucleus (Ce) exhibited the lowest labeling level since it showed only a very few number of PRV cells, even on the 3rd day post-injection.

In the diencephalon, PRV-stained cells were observed along the whole rostro-caudal extent of the hypothalamus. The hypothalamic suprachiasmatic nucleus (SCh) (Fig 2, d3) showed a few labeled cells appearing only on the third day after injection. The neurosecretory nuclei paraventricular (Pa) (Fig 2, e3) and supraoptic (SO) nuclei, also contained a moderate number of PRV cells. In the hypothalamus, the dorso- and ventro-medial nuclei (DM and VMH) (Fig 6a; Fig 2, f3), as well as the arcuate nucleus (Arc) (Fig 6a; Fig 2, g3), showed a moderate PRV staining, only on the 3rd day of injection. In the caudal part of the hypothalamus, immunocytochemical detection of calretinin allowed to delineate the parasubthalamic nucleus (PSTN) (Barbier et al., 2017) at 2 days post- injection (Fig 6b, c) (Fig 2, g2). The hypothalamus, VTM, was also infected by PRV at 2 days post-injection (Fig 2, g2), however the number of stained-cells was very scarce. Among all the hypothalamic areas, it can be underlined that the lateral area (LH) was the most labeled area (Fig 6A; Fig 2, e2, e3), suggesting a large number of indirect projections onto the MOB.

This article is protected by copyright. All rights reserved.

Dorsally to the hypothalamus, PRV- labeling was noted in the midline thalamic nuclei on the 2nd post-injection day (Fig 2, d2, e2), and became substantial on the 3rd day. Among these nuclei, the thalamic paraventricular nucleus (PV) showed the highest PRV staining.

In the epithalamus, the lateral habenula (LHb) exhibited a moderate number of PRV cells that occurred only on the 3rd day after injection while no staining was noticed in the medial habenula (Fig 2, f3).

In the ventral hippocampus, PRV- labeling appeared as soon as 2 days post-injection (Fig 2, h2, i2). By contrast, in the dorsal hippocampus the labeling occurred only on the 3rd day post injection (Fig 2, e3).

In the mesencephalon, PRV staining was noted in the VTA on the 2nd post-injection day (Fig 2, i2), and the number of labeled cells became substantial on the 3rd day (Fig 7a; Fig.2, i3).

In the brainstem, labeling occurred in the dorsal raphe nucleus (DR) (Fig 7b) as soon as the 2nd day post-injection. Only on the 3rd post-injection day, a few number of labeled cells were observed in the periaqueductal gray matter (PAG) (Fig 2, k3), and a substantial number of PRV labeled cells were also noted in the latero-dorsal tegmental nucleus (LDT) (Fig 7c; Fig 2, l3).

In the ventral part of the brainstem, a very low number of PRV-labeled cells were noted in the nucleus of the solitary tract (Sol) (Fig 2, n3) (Fig 8a). Using TH-immunocytochemical detection, we identified the noradrenergic A2 and adrenergic C2 neurons of the nucleus of the solitary tract. However, the PRV-positive neurons in the Sol were not TH-immunostained (Figs 8b, b1, b2). TH-immunostained neurons were observed in the noradrenergic A1 and adrenergic C1 of the rostral ventrolateral medulla oblongata (RVLM). In the C1 area, neurons were immunostained for both TH and PRV 152 (Figs 8c, c1, c2, Fig 2, n3).

4. DISCUSSION

Feeding behavior is under the control of complex processes involving both homeostatic and hedonic circuits. Homeostasis is based on the metabolic state when energy depletion increases the drive to eat. Meanwhile, hedonic processes are linked to the sensory properties of food and

This article is protected by copyright. All rights reserved.

reward. Olfaction plays a key part in these processes since changes in the internal state (hunger/satiety) influence the hedonic value of odors (Palouzier-Paulignan et al., 2012). In this paper we gave a general description of the indirect projections onto the MOB by using transsynaptic PRV 152 viruses. Our aim was not to quantify the retrogradely labeled neurons accurately, but to draw a map of direct projections using the CTb or indirect projections using PRV 152. Moreover, we performed injections of a limited volume of tracers (to avoid contamination of AOB and AON), therefore our results could not be used for accurate quantitative analysis. These results will be described in regards to the modulation of olfactory processing by food intake. Figure 9 synthesizes our main results.

4.1. Direct projections to the MOB

In this study we used CTb as a control as PRV 152 stained direct and indirect projections. Only considering time of migration is not sufficient to differentiate with certainty direct from indirect projections. The use of CTb allows such discrimination, as according to the literature (Luppi et al., 1990) CTb only stains direct projections. Thus, areas only stained with PRV, and not CTb, could be considered to send indirect projections to the MOB.

In addition to the confirmation of well-known projections, the present study demonstrated projections that had previously not been described. Indeed, we provided anatomical evidence of a direct projection from the VP and VTA to the MOB. It is noteworthy that the present study reports projections that seem to have been overlooked by other studies over the last few decades. Thus, several authors (Shipley & Adamek, 1984; Shipley & Ennis 1996) did not report projections neither from VTA to MOB nor from Substantia Nigra to MOB. However this does not prove their absence. Höglinger et al., (2015) demonstrated a projection from Substantia Nigra to the MOB but not from VTA to MOB. Here, we observed few cells in the VTA but not in the SN. This only indicates that dopaminergic projections to the MOB are small, and that the size and the position of tracer injections could allow them to be identified or not. This means that our data, and that of the literature, are not in opposition – especially with Höglinger's results - but complementary.

This article is protected by copyright. All rights reserved.

To date, the VP connection to the MOB has only been supported by electrophysiological data (Barragán & Ferreyra-Moyano, 1988). The VP might be implicated in reward and motivation (Castro, Cole, & Berridge, 2015). Moreover, CTb labeled cells were observed in the VTA which is a key region involved in motivation and reward-related behaviors (Fields et al., 2007). The CTb retrogradely labeled cells were TH-positive, leading us to assume that the projection from the VTA to the MOB might be dopaminergic. Thus, our tracing study indicates that regions from the reward brain circuit (e.g. VP and VTA) might modulate directly the hedonic value of food odors.

Moreover, our data went on to show for the first time direct projections to the MOB arising from the VTM nucleus of the hypothalamus which might participate in the modulation of odor processing according to feeding state and arousal level (Ericson, Blomqvist, & Kohler, 1991; Lee, Lee, & Lee, 2015). In addition, we showed that some neurons in the LH were double-labeled for both CTb and MCH. This direct MCH-projection to the MOB might play a role in feeding and stimulus-reward association (González et al., 2016). We further observed in LH some double-labeled cells for both CTb and Orx, in agreement with studies that have previously observed bulbar orexinergic fibers in rats (Peyron et al., 1998) and mice (Gascuel et al., 2012). Orexinergic neurons are involved in the regulation of feeding behavior, energy balance, and sleep-wake cycle (Sakurai et al., 1998; Sakurai, Mieda, & Tsujino, 2010). Thus, through the MCH- and Orx-projections, the LH is well-placed to modulate behavioral responses triggered by food odors depending on the metabolic status (Stuber & Wise, 2016). Here, some of the LH neurons projecting to the MOB were neither Orx nor MCH positive, and their nature remains to be elucidated

To sum up, we showed that the MOB is the target of direct projections arising from either reward or homeostatic related regions. It is known that regions such as LH and VTA are connected (Bernardis & Bellinger, 1996), suggesting that the centrifugal projections to the MOB might act in concert to change the rewarding value of a given food depending on satiety.

In addition to these new anatomical findings, our tracing study confirmed that all the primary olfactory regions (Pir, NLOT, ACo, DLEnt (Scalia & Winans, 1975; Shipley & Adamek, 1984),

This article is protected by copyright. All rights reserved.

except the Tu (in ‘t Zandt et al., 2019), send direct centrifugal fibers to the MOB. Thus in the TT, CTb staining was confined to the dorsal part, as underlined by Shipley & Ennis (1996). The transitional zone between the ventral part of the piriform cortex and the anterior cortical nucleus of the amygdala, called the cortex-amygdala transition, also showed CTb staining in accordance with a previous study (Cádiz-Moretti, Abellán-Álvaro, Pardo-Bellver, Martínez-García, & Lanuza, 2016). We also confirmed a direct projection to the MOB arising only from the CA1 subdivision of the ventral hippocampus (Van Groen & Wyss, 1990) which might be involved in the processing of fear-related odors (Fanselow & Dong, 2010; Hawley, Morch, Christie, & Leasure, 2012). As previously described, neuromodulatory projections from the MCPO/HDB (Zaborszky, Carlsen, Brashear, & Heimer, 1986), from the DR (Shipley & Adamek, 1984; Steinfeld, Herb, Sprengel, Schaefer, & Fukunaga, 2015) and from the LC (Guevara-Aguilar, Donatti-Albarran, Solano-Flores, & Wayner, 1987) were observed. TH- and 5-HT- positive cells were identified in LC and RD as these brain regions are known to send noradrenergic and serotonergic projections respectively (McLean et al., 1989, Aston-Jones & Waterhouse, 2016).

4.2. Indirect projections to the MOB

Polysynaptic tracing showed that a wide range of PRV-labeled cells were localized in limbic regions and brain reward circuits (Fig 9). As such, the Acb as a hedonic hotspot displayed PRV infected cells, as well as LHb known to be involved in the regulation of motivated behaviors including feeding (Sutherland, 1982), and in the consumption of palatable/caloric reward (Stamatakis et al., 2016). A noticeable PRV labeling was also observed in the LDT that regulates reward processing (Xiao et al., 2016). Furthermore, the PT gave rise to indirect projections which play a role in food anticipatory behavior in the case of intermittent food access (Nakahara et al., 2004), and in the modulation of arousal states linked with appetitive emotional valence (Kirouac, 2015). Here, we also reported that the BLA is also a source of indirect projections to the MOB. The BLA receives information from multiple sensory modalities including olfaction. The BLA encodes significant stimuli, and seems critical in the formation of memories of both positive and negative odor valence (Cardinal, Parkinson, Hall, & Everitt, 2002; Sevelinges, Lévy, Mouly, & Ferreira, 2009). All these regions (Acb, LHb,

This article is protected by copyright. All rights reserved.

LDT, PVT and BLA) have connections with the VTA, and subsequently participate in the brain reward circuitry (Steidl & Veverka, 2015).

Analysis of the neocortical areas showed PRV labeling in the infralimbic cortex (IL). The IL has been shown to modulate the visceral responses to sensory stimuli (Hurley, Herbert, Moga, & Saper, 1991), and the integration of aversive emotional experience (Kincheski, Mota-Ortiz, Pavesi, Canteras, & Carobrez, 2012). Indirect projections to the MOB also originated from the AI, considered as a convergence region of both olfactory and visceral pathways underlying food selection and memory (Dardou, Datiche, & Cattarelli, 2006). Lastly, the LO/VLO involved in decision–making and the regulation of behavioral responses exhibited PRV cells. It has been shown that both orbital and insular cortices participate to the hedonic responses toward sensory rewards, such as 'liking' for sweetness (Castro & Berridge, 2017).

A substantial PRV labeling was also noticed in the Re which projects to the hippocampal CA1 subfield (Vertes, Linley, & Hoover, 2015) and to the Pir (Datiche, Luppi, & Cattarelli, 1995). The hippocampus-reuniens-cortical network may be important for the consolidation of olfactory memory traces during exploratory behavior (Varela, Kumar, Yang, & Wilson, 2014). Thus, rodents routinely forage to find sources of caloric food in their environment, and this behavior might rely on hippocampal-dependent spatial memory (Kulkarni, Stolberg, Sullivan Jr., & Ferris, 2012; Aqrabawi et al., 2016).

In the hypothalamus, some PRV-labeled cells were noticed in nuclei that participate in metabolic regulation of food intake such as the Arc, the VMH and the DM. Hence, the Arc receives signals from the digestive system (Elias et al., 1999) and is a key region in the regulation of appetite (Chen, Lin, Kuo, & Knight, 2015). The VMH is known as the primary satiety center (Ahima & Antwi, 2008), and the DM plays a role in body-weight regulation (Bellinger & Bernardis, 2002).

Analysis of the dorsal part of the brainstem indicated that the Sol sends indirect projections to the MOB. The Sol is involved in both sensory and visceral integration, and participates in the

This article is protected by copyright. All rights reserved.

regulation of energy balance (Grill & Hayes, 2012). This nucleus is in a key position for the transmission of orosensory information to higher sensory brain regions which will elaborate adequate behavioral and/or physiological responses. Our study demonstrated that PRV neurons were also labeled for TH in the Sol, suggesting an indirect catecholaminergic modulation of odor processing. It needs to be pointed out that the caudal Sol contains noradrenergic A2 neurons sending projections onto the mesolimbic reward system, including the VTA and the Acb (Martin et al., 2009). Thus, the Sol might also be considered as an essential interface between the brain network that integrates energy status/metabolic signals and brain network that controls hedonic aspects of feeding behavior (Grill & Hayes, 2012).

In the brainstem, we also showed double-labeled cells for both TH and PRV in the C1 area of the RVLM, a region invovled in various autonomic responses such as glucoprivic responses (Abbott et al., 2013).

Taken together, our tracing study demonstrated that the MOB receives widespread indirect projections originating from regions which are more or less involved in hedonic or homeostatic networks, or both (Fig 9). Our data support the idea that odor processing at the MOB level can be modulated by several pathways belonging to homeostatic and/or hedonic circuits that will allow adaptation of food intake and food choices. More generally, our study indicates that complex behavior such as feeding clearly relies on complex chains of connected neurons in the brain.

This article is protected by copyright. All rights reserved.

References

Abbott, S.B.G., DePuys, S.D. Nguyen, T., Coates, M., Stornetta, R.L., & Guyenet, P.G. 2013. Selective optgenetic activation of rostral ventrolateral medullary catecholaminergic neurons produces cardiorespiratory stimulation in conscious mice. *J. Neurosci.* 33(7):3164-3177.

Ahima, R. S., & Antwi, D. A. (2008). Brain Regulation of Appetite and Satiety. *Endocrinology and Metabolism Clinics of North America*, 37(4), 811–823. http://doi.org/10.1016/j.ecl.2008.08.005

Aqrabawi, A., Browne, C., Dargaei, Z., Garand, D., Khademullah, C., Woodin, M., & Kim, J. (2016). Top-down modulation of olfactory-guided behaviours by the anterior olfactory nucleus pars medialis and ventral hippocampus. *Nature Communications*, 7(13721), 1–9. http://doi.org/10.1038/ncomms13721

Aston-Jones, G., & Waterhouse, B. (2016). Locus coeruleus: From global projection system to adaptive regulation of behavior. *Brain Research*, 1645, 75–78. http://doi.org/10.1016/j.brainres.2016.03.001

Barbier, M., Chometon S., Peterschmitt, Y., Fellmann, D., Risold, PY. (2017). Parasubthalamic and Calbindin nuclei in the posterior lateral hypothalamus are the major hypothalamic target for projections from the central and anterior basomedial nuclei of amygdala. Brain Struct. Funct. 222:2961-2991.

Barragán, E., & Ferreyra-Moyano, H. (1988). Electrophysiological connections of neurons in ventral pallidal regions of the olfactory tubercle with the main olfactory bulb and piriform cortex. *Neuroscience Letters*, 93(2–3), 214–219. http://doi.org/10.1016/0304-3940(88)90084-5

Bellinger, L. L., & Bernardis, L. L., 2002. The dorsomedial hypothalamic nucleus and its role in ingestive behavior and body weight regulation: Lessons learned from lesioning studies. *Physiology & Behavior*. 76(3):431-432.

Bernardis, L. L., & Bellinger, L. L. (1996). The lateral hypothalamic area revisited: ingestive behavior. *Neuroscience and Biobehavioral Reviews*, 20(2), 189–287. http://doi.org/10.1016/0149-7634(95)00015-1

Boldogköi, Z., Sík, A., Dénes, Á., Reichart, A., Toldi, J., Gerendai, I., … Palkovits, M. (2004). Novel tracing paradigms - Genetically engineered herpes viruses as tools for

This article is protected by copyright. All rights reserved.

mapping functional circuits within the CNS: Present status and future prospects. *Progress in Neurobiology*, 72(6), 417–445. http://doi.org/10.1016/j.pneurobio.2004.03.010

Boyd, A. M., Sturgill, J. F., Poo, C., & Isaacson, J. S. (2012). Cortical feedback control of olfactory bulb Circuits. *Neuron*, 76(6), 1161–1174. http://doi.org/10.1016/j.neuron.2012.10.020

Cádiz-Moretti, B., Abellán-Álvaro, M., Pardo-Bellver, C., Martínez-García, F., & Lanuza, E. (2016). Afferent and efferent connections of the cortex-Amygdala transition zone in mice. *Frontiers in Neuroanatomy*, 10, 1–18. http://doi.org/10.3389/fnana.2016.00125

Canetti, L., Bachar, E., & Berry, E. M. (2002). Food and emotion. *Behavioural Processes*, 60(2), 157–164. http://doi.org/10.1016/S0376-6357(02)00082-7

Cardinal, R. N., Parkinson, J. A., Hall, J., & Everitt, B. J. (2002). Emotion and motivation: the role of the amygdala, ventral striatum, and prefrontal cortex. *Neuroscience & Biobehavioral Reviews*, 26(3), 321–352. http://doi.org/10.1016/S0149-7634(02)00007-6

Castro, D.C., & Berridge, K.C. (2017). Opioid and orexin hedonic hotspot in rat orbitofrontal cortex and insula. *Proc. Natl. Acad. Sci. U.S.A.* 114(43):E9125-E9134. https://doi.org/10.1073/pnas.1705753114

Castro, D. C., Cole, S. L., & Berridge, K. C. (2015). Lateral hypothalamus, nucleus accumbens, and ventral pallidum roles in eating and hunger: interactions between homeostatic and reward circuitry. *Frontiers in Systems Neuroscience, 9:* 1–17. http://doi.org/10.3389/fnsys.2015.00090

Celio, M.R. 1990. Calbindin D-28K and parvalbumin in the rat nervous system. *Neuroscience.* 35:375-475.

Chen, Y., Lin, Y. C., Kuo, T. W., & Knight, Z. A. (2015). Sensory detection of food rapidly modulates arcuate feeding circuits. *Cell*, 160(5), 829–841. http://doi.org/10.1016/j.cell.2015.01.033

Dardou, D., Datiche, F., & Cattarelli, M. (2006). Fos and Egr1 expression in the rat brain in response to olfactory cue after taste-potentiated odor aversion retrieval. *Learning & Memory*, 13(2), 150–60. http://doi.org/10.1101/lm.148706

Datiche, F., Luppi, P. N., & Cattarelli, M. (1995). Projection from nucleus reuniens thalami to piriform cortex: A tracing study in the rat. *Brain Research Bulletin*, 38(1), 87–92. http://doi.org/10.1016/0361-9230(95)00075-P

This article is protected by copyright. All rights reserved.

Duclaux, R., Feisthauer, J., & Cabanac, M. (1973). Effets du repas sur l'agrément d'odeurs alimentaires et non alimentaires chez l'homme, *Physiology & Behavior*, 10, 1029–1033.

Elias, C. F., Aschkenasi, C., Lee, C., Kelly, J., Ahima, R. S., Bjorbæk, C., & Elmquist, J. K. (1999). Leptin differentially regulates NPY and POMC neurons projecting to the lateral hypothalamic area. *Neuron*, 23(4), 775–786. http://doi.org/10.1016/S0896-6273(01)80035-0

Enquist, L. W., & Card, J. P. (2003). Recent advances in the use of neurotropic viruses for circuit analysis. *Current Opinion in Neurobiology*, 13(5), 603–606. http://doi.org/10.1016/j.conb.2003.08.001

Ericson, H., Blomqvist, A., & Kohler, C. (1991). Origin of neuronal inputs to the region of the tuberomammillary nucleus of the rat brain. *Journal of Comparative Neurology*, 311(1), 45–64. http://doi.org/10.1002/cne.903110105

Fanselow, M.S., Dong, H. 2010. Are the dorsal and ventral hippocampus functionally distinct structures? *Neuron* 65(1):7-19.

Fields, H.L., Hjelmstad, G.O., Margolis , E.B., Nicola, S.M. 2007. Ventral tegmental area neurons in learned appetitive behavior and positive reinforcement. *Annu. Rev. Neurosci.* 30:289-316.

Franklin, K.B.J., Paxinos, G, 2007. The mouse Brain in stereotaxic coordinates (3rd ed.) Amsterdam: Elsevier Academic.

Gascuel, J., Lemoine, A., Rigault, C., Datiche, F., Benani, A., Pénicaud, L., & Lopez-Mascaraque, L. (2012). Hypothalamus-olfactory system crosstalk: orexin a immunostaining in mice. *Frontiers in Neuroanatomy*, 6, (44)1-11. http://doi.org/doi: 10.3389/fnana.2012.00044

González, J. A., Iordanidou, P., Strom, M., Adamantidis, A., Burdakov, D., & Figure, S. (2016). Awake dynamics and brain-wide direct inputs of hypothalamic MCH and orexin networks. *Nature Communications*, 7(c), 11395. http://doi.org/10.1038/ncomms11395

Grill, H. J., & Hayes, M. R. (2012). Hindbrain neurons as an essential hub in the neuroanatomically distributed control of energy balance. *Cell Metabolism*, 16(3), 296–309. http://doi.org/10.1016/j.cmet.2012.06.015

Guevara-Aguilar, R., & Aguilar-Baturoni, H. U. (1978). Olfactory pathway evoked potentials in response to hypothalamic stimulation. *Brain Research Bulletin*, 3(5), 467–474. http://doi.org/10.1016/0361-9230(78)90076-X

This article is protected by copyright. All rights reserved.

Guevara-Aguilar, R., Donatti-Albarran, O. A., Solano-Flores, L. P., & Wayner, M. J. (1987). Nucleus of the tractus solitarius projections to the olfactory tubercle: An HRP study. *Brain Research Bulletin*, 18(5), 673–675. http://doi.org/10.1016/0361-9230(87)90138-9

Hawley, D. F., Morch, K., Christie, B. R., & Leasure, J. L. (2012). Differential response of hippocampal subregions to stress and learning. *PLoS ONE*, 7(12) e53126. http://doi.org/10.1371/journal.pone.0053126

Hintiryan, H., Gou, L., Zingg, B., Yamashita, S., Lyden, H. M., Song, M. Y., … Dong, H.-W. (2012). Comprehensive connectivity of the mouse main olfactory bulb: analysis and online digital atlas. *Frontiers in Neuroanatomy*, 6*:* 1–16. http://doi.org/10.3389/fnana.2012.00030

Höglinger, G. U., Alvarez-Fischer, D., Arias-Carrión, O., Djufri, M., Windolph, A., Keber, U., … Oertel, W. H. (2015). A new dopaminergic nigro-olfactory projection. *Acta Neuropathologica*, 130(3), 333–348. http://doi.org/10.1007/s00401-015-1451-y

Hurley, K. M., Herbert, H., Moga, M. M., & Saper, C. B. (1991). Efferent Projections of the Infralimbic Cortex of the Rat. *The Journal of Comparative Neurology*, 308(2):249-276. http://doi.org/10.1002/cne.903080210

In ‘t Zandt, E.E., Cansler, H.L., Denson, H.B., Wesson,D.W. (2019). Centrifugal innervation of the olfactory bulb: A reappraisal. eNeuro6(1) e0390-18.2019: 1-12

Kincheski, G. C., Mota-Ortiz, S. R., Pavesi, E., Canteras, N. S., & Carobrez, A. P. (2012). The dorsolateral periaqueductal gray and its role in mediating fear learning to life threatening events. *PLoS ONE*, 7(11):e50361. http://doi.org/10.1371/journal.pone.0050361

Kirouac, G. J. (2015). Placing the paraventricular nucleus of the thalamus within the brain circuits that control behavior. *Neuroscience and Biobehavioral Reviews*, 56, 315–329. http://doi.org/10.1016/j.neubiorev.2015.08.005

Kulkarni, P., Stolberg, T., SullivanJr., J. M., & Ferris, C. F. (2012). Imaging evolutionarily conserved neural networks: Preferential activation of the olfactory system by food-related odor. *Behavioural Brain Research*, 230(1), 201–207. http://doi.org/10.1016/j.bbr.2012.02.002

Lee, J. S., Lee, E. Y., & Lee, H. S. (2015). Hypothalamic, feeding/arousal-related peptidergic projections to the paraventricular thalamic nucleus in the rat. *Brain Research*, 1598, 97–113. http://doi.org/10.1016/j.brainres.2014.12.029

Luppi, P.H., Fort, P., & Jouvet, M. (1990). Iontophoretic application of unconjugated cholera

This article is protected by copyright. All rights reserved.

toxin B subunit (CTb) combined with immunohistochemistry of neurochemical substances: a method for transmitter identification of retrogradely labeled neurons. *Brain Research,* 26; 534(1-2):209-224.

Martin, F., Laorden, M.L., Milanes, M. V. 2009. Morphin withdrawal regulates phosphorylation of cAMP responses elements binding protein (CREB) through PKC in the nucleus tractus solitarius- A2 catecholaminergic neurons. *J. Neurochem.* 110(5):1422-1432

Matsutani, S., & Yamamoto, N. (2008). Centrifugal innervation of the mammalian olfactory bulb. *Anatomical Science International*, *83*(4), 218–227. http://doi.org/10.1111/j.1447-073x.2007.00223.x

McLean JH, Shipley MT, Nickell WT, Aston-Jones G, Reyher CK. Chemoanatomical organization of the noradrenergic input from locus coeruleus to the olfactory bulb of the adult rat. J Comp Neurol. 1989;285(3):339–349.

Miyamichi, K., Amat, F., Moussavi, F., Wang, C., Wickersham, I., Wall, N. R., … Luo, L. (2011). Cortical representations of olfactory input by trans-synaptic tracing. *Nature*, 472(7342), 191–196. http://doi.org/10.1038/nature09714

Nakahara, K., Fukui, K., Murakami, N., 2004. Involvement of thalamic paraventricular nucleus in the anticipatory reaction under food restriction in the rat. *J. Vet. Med. Sci.* 66(10):1297-1300.

Pager, J., Giachetti, I., Holley, A., & Le Magnen, J. (1972). A selective control of olfactory bulb electrical activity in relation to food deprivation and satiety in rats. *Physiology & Behavior*, 9(4), 573–579. http://doi.org/10.1016/0031-9384(72)90014-5

Palouzier-paulignan, B., Lacroix, M. C., Aimé, P., Baly, C., Caillol, M., Congar, P., … Fadool, D. A. (2012). Olfaction under metabolic influences. *Chemical Senses*, 37(9), 769–797. http://doi.org/10.1093/chemse/bjs059

Peyron, C., Tighe, D. K., van den Pol, a N., de Lecea, L., Heller, H. C., Sutcliffe, J. G., & Kilduff, T. S. (1998). Neurons containing hypocretin (orexin) project to multiple neuronal systems. *The Journal of Neuroscience : The Official Journal of the Society for Neuroscience*, 18(23), 9996–10015. http://doi.org/10.1.1.335.5389

Rolls, B. J., Rolls, E. T., Rowe, E. A., & Sweeney, K. (1981). Sensory specific satiety in man. *Physiology and Behavior*, 27(1), 137–142. http://doi.org/10.1016/0031-9384(81)90310-3

Sakurai, T., Amemiya, A., Ishii, M., Matsuzaki, I., Chemelli, R. M., Tanaka, H., … Yanaqisawa, M.(1998). Orexins and Orexin Receptors: A Family of Hypothalamic

This article is protected by copyright. All rights reserved.

Neuropeptides and G Protein-Coupled Receptors that Regulate Feeding Behavior. *Cell*, 92, 573–585. http://doi.org/10.1016/S0092-8674(00)80949-6

Sakurai, T., Mieda, M., & Tsujino, N. (2010). The orexin system: Roles in sleep/wake regulation. *Annals of the New York Academy of Sciences*, 1200, 149–161. http://doi.org/10.1111/j.1749-6632.2010.05513.x

Scalia, F., Winans, S. S. (1975). The differential projections of the olfactory bulb and accessory olfactory bulb in mammals. *Journal of Comparative Neurology*. 161(1):31-55.

Shipley, M.T., Ennis, M. (1996). Functional organization of olfactory system. *J. Neurobiol*. 30:123-176.

Shipley, M. T., & Adamek, G. D. (1984). The connections of the mouse olfactory-bulb - a study using orthograde and retrograde transport of wheat-germ-agglutinin conjugated to horseradish-peroxidase. *Brain Research Bulletin*, 12(6), 669–688. http://doi.org/10.1016/0361-9230(84)90148-5

Sevelinges, Y., Lévy, F., Mouly, A.-M., & Ferreira, G. (2009). Rearing with artificially scented mothers attenuates conditioned odor aversion in adulthood but not its amygdala dependency. *Behavioural Brain Research*, 198(2), 313–320. http://doi.org/10.1016/j.bbr.2008.11.003

Smith, G.A., Enquist, L.W., 2000. A self-recombining bacterial artificial chromosome and its application for analysis of herpesvirus pathogenesis. *Proc. Natl. Acad. Sci. U.S.A.* 97, 4873–4878.

Stamatakis, A. M., Van Swieten, M., Basiri, M. L., Blair, G. A., Kantak, P., & Stuber, G. D. (2016). Lateral Hypothalamic Area Glutamatergic Neurons and Their Projections to the Lateral Habenula Regulate Feeding and Reward. *Journal of Neuroscience*, 36(2), 302–311. http://doi.org/10.1523/JNEUROSCI.1202-15.2016

Steidl, S., & Veverka, K. (2015). Optogenetic excitation of LDTg axons in the VTA reinforces operant responding in rats. *Brain Research*, 1614, 86–93. http://doi.org/10.1016/j.brainres.2015.04.021

Steinfeld, R., Herb, J. T., Sprengel, R., Schaefer, A. T., & Fukunaga, I. (2015). Divergent innervation of the olfactory bulb by distinct raphe nuclei. *Journal of Comparative Neurology*, 523(5), 805–813. http://doi.org/10.1002/cne.23713

Stuber, G. D., & Wise, R. A. (2016). Lateral hypothalamic circuits for feeding and reward. *Nature Neuroscience*, 19(2), 198–205. http://doi.org/10.1038/nn.4220

This article is protected by copyright. All rights reserved.

Sutherland, R. J. (1982). The dorsal diencephalic conduction system: A review of the anatomy and functions of the habenular complex. *Neuroscience & Biobehavioral Reviews*, 6(1), 1–13. http://doi.org/10.1016/0149-7634(82)90003-3

Van Groen, T., & Wyss, J. M. (1990). Extrinsic projections from area CA1 of the rat hippocampus: Olfactory, cortical, subcortical, and bilateral hippocampal formation projections. *Journal of Comparative Neurology*, 302(3), 515–528. http://doi.org/10.1002/cne.903020308

Varela, C., Kumar, S., Yang, J. Y., & Wilson, M. A. (2014). Anatomical substrates for direct interactions between hippocampus, medial prefrontal cortex, and the thalamic nucleus reuniens. *Brain Structure and Function*, 219(3), 911–929. http://doi.org/10.1007/s00429-013-0543-5

Vertes, R. P., Linley, S. B., & Hoover, W. B. (2015). Limbic circuitry of the midline thalamus. *Neuroscience and Biobehavioral Reviews*, 54, 89–107. http://doi.org/10.1016/j.neubiorev.2015.01.014

Wen, P., Rao, X., Xu, L., Zhang, Z., Jia, F., He, X., Xu, F. (2019). Cortical organization of centrifugal afferents to the olfactory bulb: mono- and trans- synaptic tracing with recombinant neurotropic viral tracers. Neurosci Bull. DOI:.org/10.1007/s12264/019/00385-6

Xiao, C., Cho, J.R., Zhou ,C., Treweek, J.B., Chan, K., McKinney S.L., Yang, B., Gradinaru, V. 2016. Cholinergic mesopontin signals governs locomotion and reward through dissociable midbrain pathways. *Neuron*. 90(2):3333-347.

Zaborszky, L., Carlsen, J., Brashear, H. R., & Heimer, L. (1986). Cholinergic and gabaaergic afferents to the olfactory-bulb in the rat with special emphasis on the projection neurons in the nucleus of the horizontal limb of the diagonal band. *Journal of Comparative Neurology*, 243(4), 488–509.

Legend:

Figure 1.
a-c1: Controls for diffusion of PRV 152 from injections sites (a-c : Coronal sections of the MOB; Arrow : injection site; a1-c1: coronal section of the AOB and AON). No labelling was observed in the AOB showing that there was no PRV diffusion outside the MOB. The staining observed in the

This article is protected by copyright. All rights reserved.

AON was not due to diffusion, but illustrates the projections from the AON to the MOB. PRV 152 traces the chain of connected neurons including local networks. Thus this increases the staining, in contrast with CTbbelow (a, a1: Hoechst; b, b1: PRV; c, c1: Merge).
d-f1: Controls for diffusion of CTbfrom injection sites (d-f : Coronal sections of the MOB; Arrow : injection site; d1-f1: coronal sections of the AOB and AON) shows that CTbdo not spread out of the injection site. The very light staining observed in the AON was not due to diffusion, but as for PRV 152, illustrates the projections from the AON to the MOB. (d, d1: Hoechst; e, e1: CTb; f, f1: Merge).
AOB : Accessory Olfactory Bulb ; AON : Anterior Olfactory Nucleus; CGL: Granular Cell Layer

Figure 2. Antero posterior coronal sections illustrating the distribution of direct (CTb; a1 to n1) and indirect staining with PRV 152 (2 days post injection: a2 to n2; 3 days post injection a3 to n3). The last column illustrates the corresponding brain level according to the Franklin & Paxinos mouse brain atlas. Drawing result of a compilation of 4 animals for CTb, 4 for 2 days PRV and 4 for 3 days PRV.

Figure 3. a-a1: Illustration at low and higher magnification of the CTb retrograde labeling in the ventral pallidum (VP) indicating a direct projection from the VP to the MOB. b-b1: Photomicrographs depicting at low and higher magnification a retrogradely CTb stained neuron in the ventral tubero mammillary nucleus (VTM). Blue staining is Hoechst nuclear staining to visualize nucleus.
Cl : Island of Calleja; MTu: medial mammillary nucleus; PMCo: posteromedial cortical nucleus of the amygdala ; Tu : Olfactory tubercle.

Figure 5. The ventral tegmental area (VTA) showed a low number of CTb retrogradely labeled neurons. Immunohistochemical staining against tyrosine-hydroxylase (TH) showed that the CTb stained cells were TH-positive, indicating a direct monoaminergic projection from the VTA to the main olfactory bulb. a1: TH immunostaining (green), a2 : CTb immunostaining (orange), a3: merge.
IPR: interpeduncular nucleus; SNR: substantia nigra, reticular part.

Figure 6. Illustration of the distribution of the neurons labeled by PRV 152 in the hypothalamus on the 3rd post-injection day. Indirect projections onto the MOB originate from several hypothalamic regions.
a: The lateral hypothalamus (LH) showed a substantial number of retrogradely labeled neurons. In contrast, a moderate labeling was observed in other hypothalamic areas such as the dorsomedial (DM), the ventromedial (VMH) and the arcuate (Arc) nuclei. Hoechst's blue staining allows visualization of nuclei.

This article is protected by copyright. All rights reserved.

b: Low magnification of the hypothalamus at the level of the parasubthalamus nucleus (PSTN) where a noticeable number of PRV 152 stained cells were observed. c1: High magnification of the PSTN: Some neurons were double-labeled for both PRV 152 and calretinin. PRV 152 immunostaining (green); c2: Calretinin immunostaining (orange), c3: merge.
Cp: cerebral peduncle; STh: subthalamus nucleus.

Figure 7. Low and high magnification of the indirect labeling observed following PRV 152 injection into the MOB showing projections from :
a-a1: the ventral tegmental area (VTA);
b-b1: the dorsal raphe (DR)
c-c1: the laterodorsal tegmental nucleus (LDT).

Figure 8. a: Low magnification microphotograph showing the distribution of PRV 152 labeled cells in the brainstem. b: The nucleus of the solitary tract (Sol) showed some retrogradely labeled cells that were also positive for TH (B: TH staining (orange); b1: PRV staining (green); b2: merge). The rostral ventrolateral medulla oblongata (RVLM) exhibited some retrogradely labeled cells that were also positive for TH (C:TH staining (orange); c1: PRV 152 staining (green); c2: merge).
Gi: gigantocellular reticular nucleus; IRt: intermediate reticular nucleus; mlf: medial longitudinal fasciculus; SP5l: Spinal trigeminal nucleus.

Figure 9: Schematic illustration of the monosynaptic and polysynaptic centrifugal projections onto the main olfactory bulb. The injections of either CTb or PRV in the MOB granular layer were used to retrogradely trace the direct (red arrows: CTb labeling) and indirect (filled black arrow: PRV labeling 2 days-post injection; dot black arrows: PRV labeling 3 days-post injection) centrifugal projections. Analysis of the distribution of the retrogradely labeled neurons focused on feeding- related areas. In the hypothalamus, the LH sends both direct and indirect projections. All the other hypothalamic nuclei showed only polysynaptic centrifugal connections with the MOB. Among regions involved in the reward circuitry, the VTA and VP send both direct and indirect projections. The present tracing study was descriptive. Nevertheless, despite the lack of quantitative analysis, we used a thiner arrow to indicate that a low number of neurons were CTb stained. The MOB is the target of indirect projections arising from the brainstem (NTS and RVLM). See table for abbreviations.

Graphical abstract: Retrograde trans-synaptic viruses (a) allowed to trace (2-3 synapses) projections onto the main olfactory bulb (b). Monosynaptic CTb (a) was a control to differentiate direct and indirect projections. The MOB mainly receives indirect projections from hypothalamic nuclei (c) and reward-related regions (c1), underlining the role of olfaction in feeding (d).

This article is protected by copyright. All rights reserved.

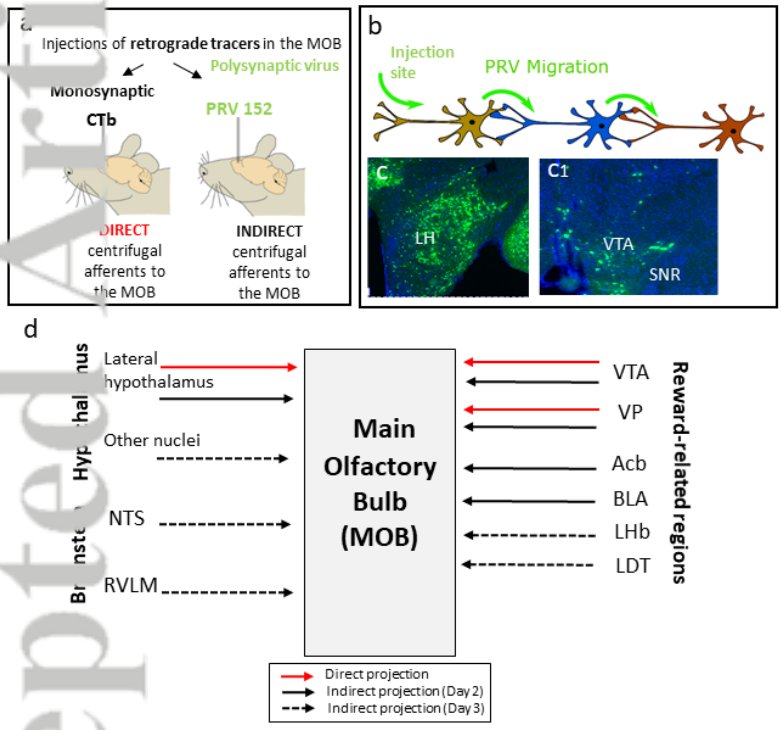

CNE_24846_Graphical abstract JCN-19-0094.R2.TIF

This article is protected by copyright. All rights reserved.

Retrograde trans-synaptic viruses (a) allowed to trace (2-3 synapses) projections onto the main olfactory bulb (b). Monosynaptic CTb (a) was a control to differentiate direct and indirect projections. The MOB mainly receives indirect projections from hypothalamic nuclei (c) and reward-related regions (c1), underlining the role of olfaction in feeding (d).

This article is protected by copyright. All rights reserved.

Primary antibody raised against	Species	dilution	Reference/source
GFP	Chicken	1 :5000	Ab 13970 abcam
CTb	Rabbit	1 :1000	AB34992 abcam
	Mouse	1 :1000	AB62769
Orexin A	Rabbit	1 :1000	AB 3098
Somatostatin	Goat	1 :500	SC7819 Santa Cruz
MCH	Rabbit	1 :1000	Personal gift PY Risold
TH	Rabbit	1:1000	calbiochem
5 HT	Rabbit	1:1000	Personal gift PY Risold
Calretinin	Rabbit	1:1000	Personal gift PY Risold
Calbindin	Mouse	1:1000	Personnal gift PY Risold
Parvalbumin	Mouse	1:1000	Personal gift PY Risold

Secondary antibody raised against	Species	Dilution	Reference/source
Chicken IgY	Goat	1:1000	AB 150169 abcam alexafluor 488
Rabbit	Donkey	1:500	AB 175694 abcam alexafluor 568
	Goat	1:700	A11001 InVitrogene alexafluor 488
	Goat	1:500	Ab11034 abcam alexafluor 488
Mouse	Goat	1:500	A 11045 alexafluor 350
	Goat	1:500	A11032 alexafluor 594
Goat	Donkey	1:1000	A 21081 Molecular Probes alexafluor 350

Table 1. List of antibodies and incubation time and concentration in the different immunohistological experiments.

This article is protected by copyright. All rights reserved.

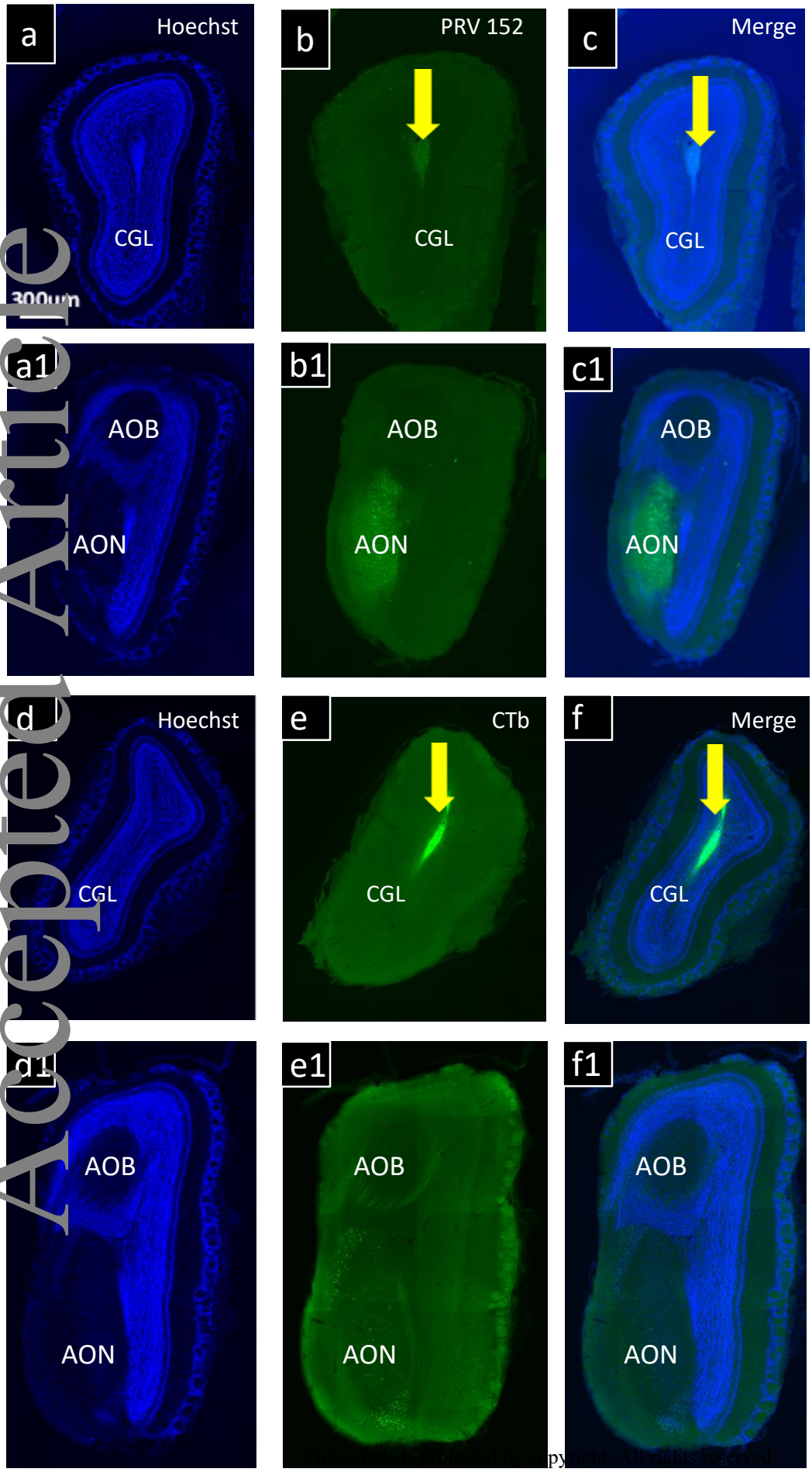

Figure 1.

a-c1: Controls for diffusion of PRV 152 from injections sites (a-c : Coronal sections of the MOB; Arrow : injection site; a1-c1: coronal section of the AOB and AON). No labelling was observed in the AOB showing that there was no PRV diffusion outside the MOB. The staining observed in the AON was not due to diffusion, but illustrates the projections from the AON to the MOB. PRV 152 traces the chain of connected neurons including local networks. Thus this increases the staining, in contrast with CTb below (a, a1: Hoechst; b, b1: PRV; c, c1: Merge).

d-f1: Controls for diffusion of CTb from injection sites (d-f : Coronal sections of the MOB; Arrow : injection site; d1-f1: coronal sections of the AOB and AON) shows that CTb do not spread out of the injection site. The very light staining observed in the AON was not due to diffusion, but as for PRV 152, illustrates the projections from the AON to the MOB. (d, d1: Hoechst; e, e1: CTb; f, f1: Merge).

AOB : Accessory Olfactory Bulb ; AON : Anterior Olfactory Nucleus; CGL: Granular Cell Layer

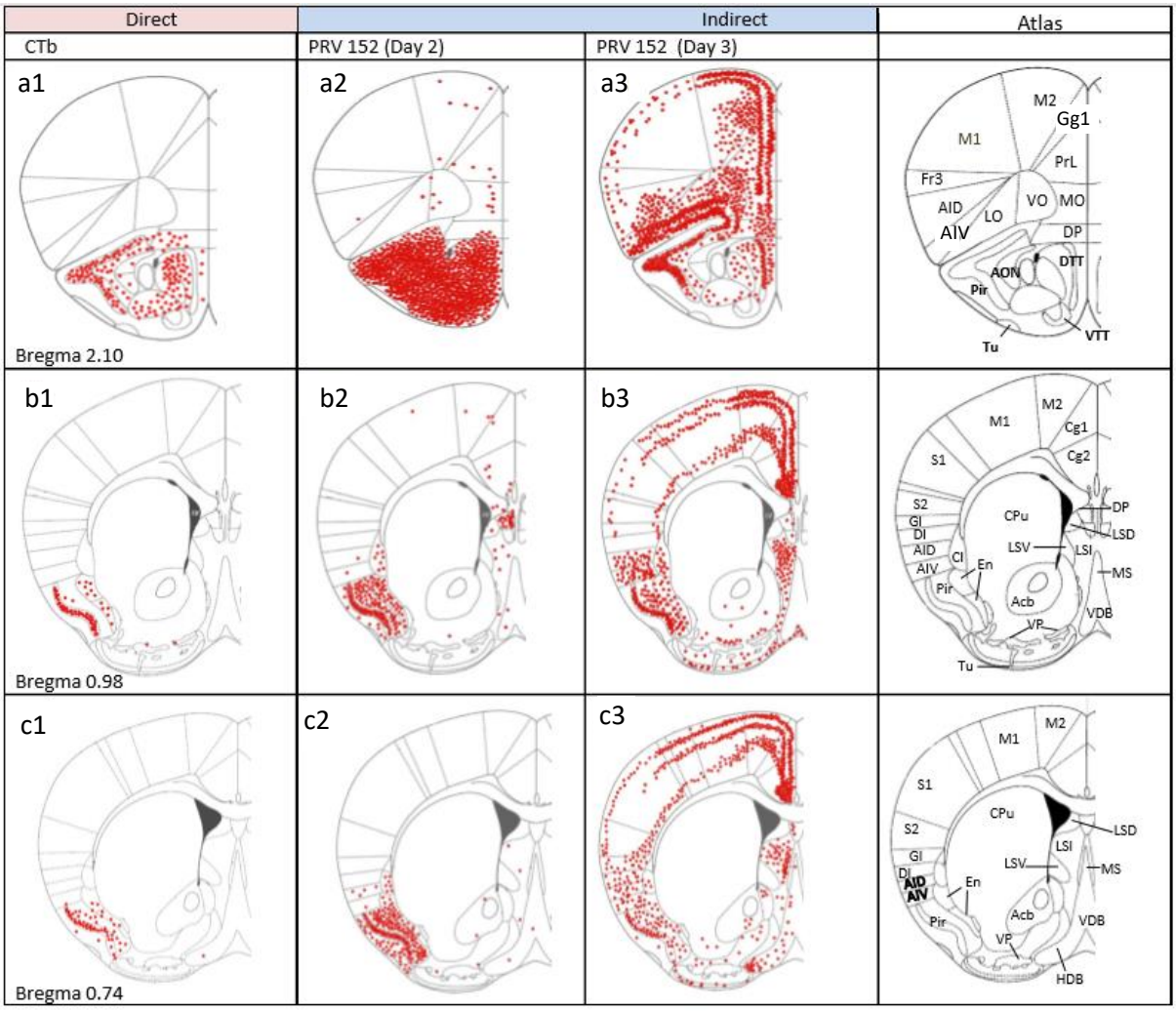

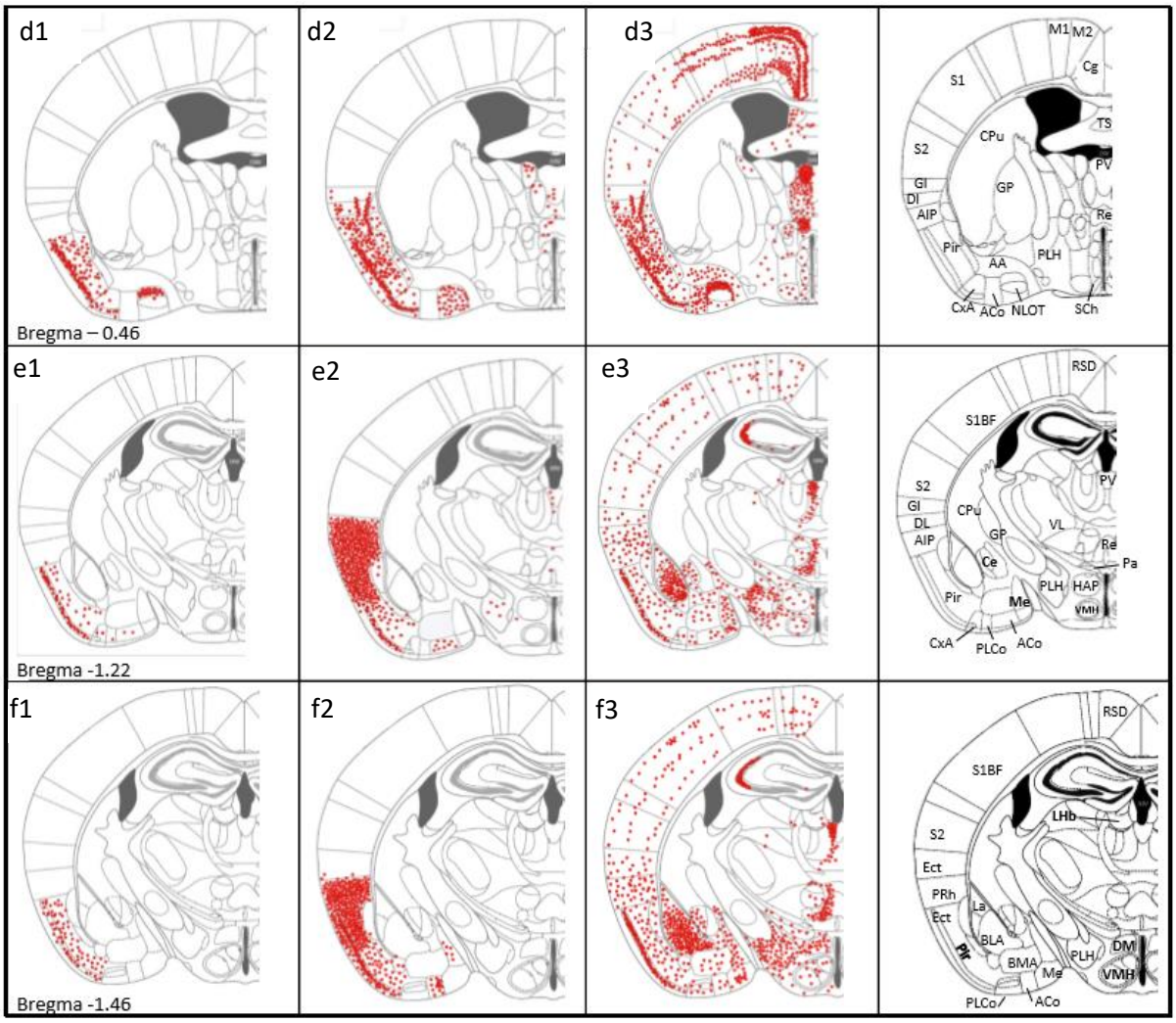

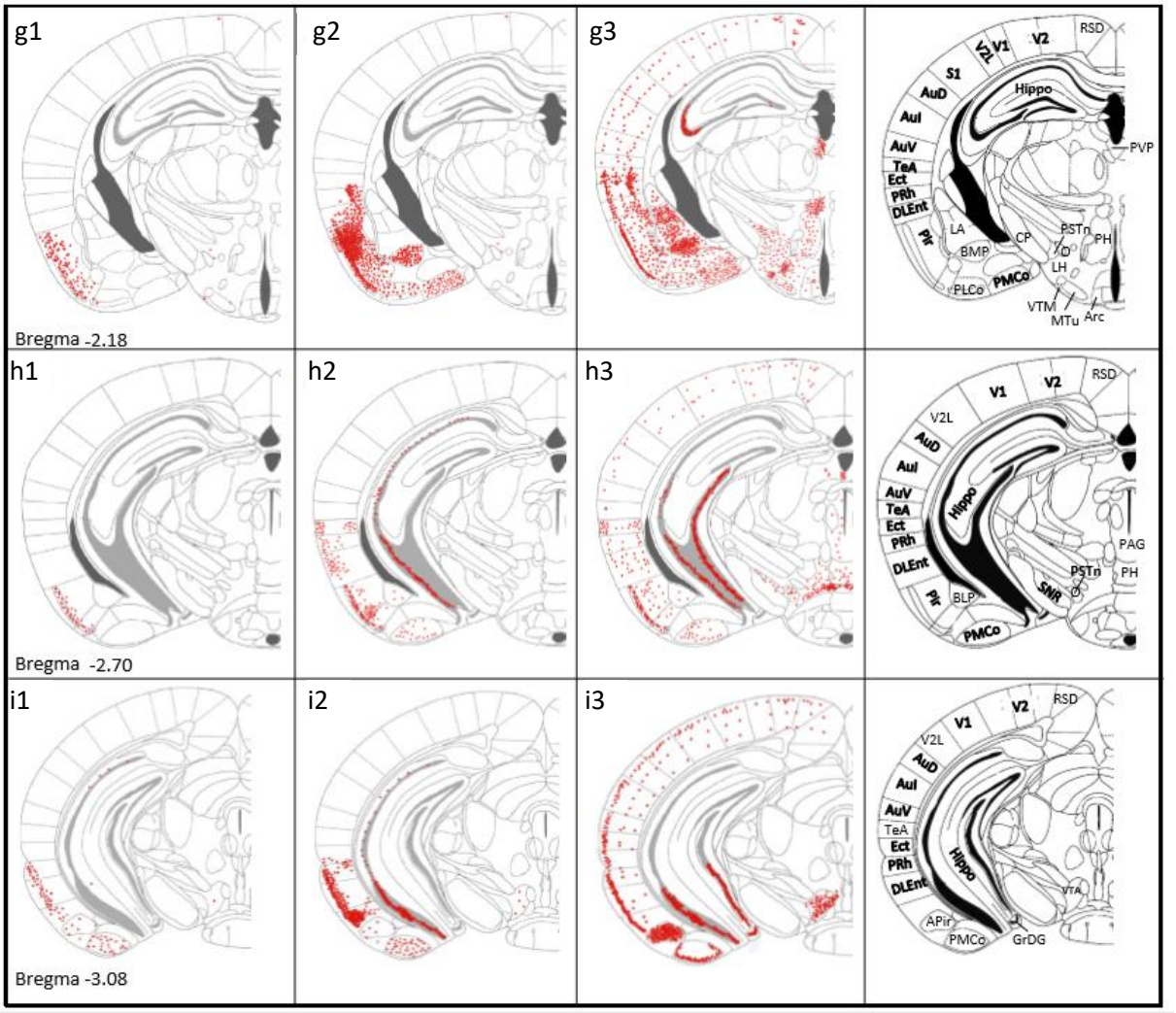

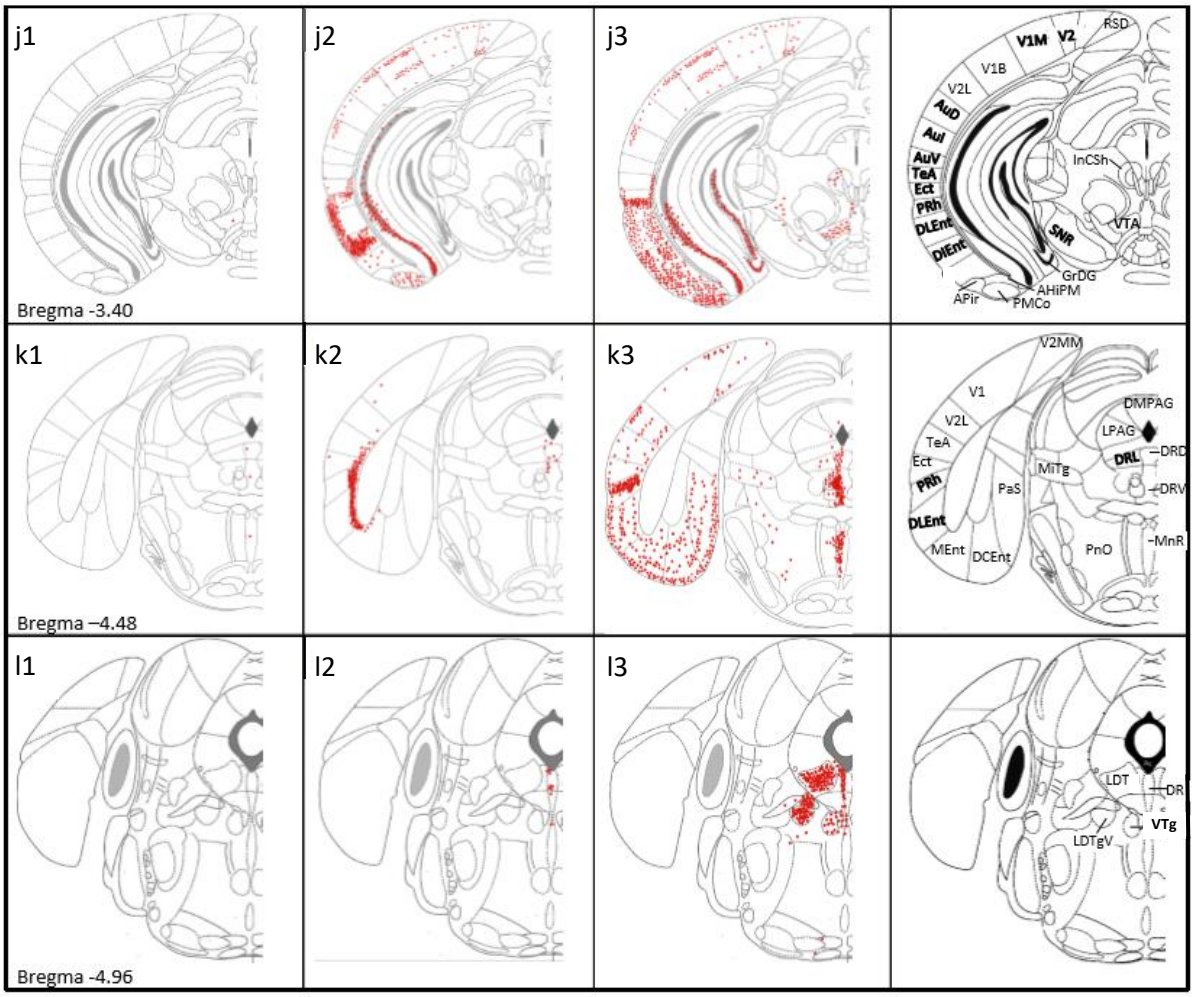

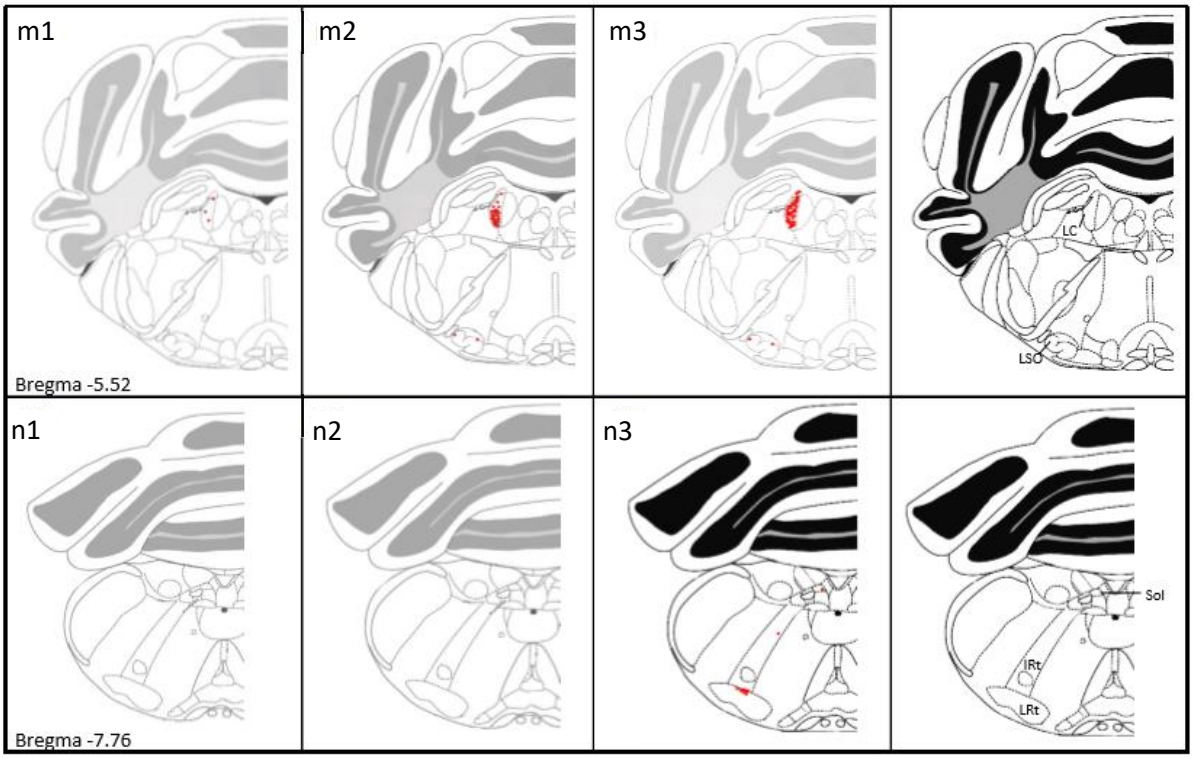

Figure 2. Antero posterior coronal sections illustrating the distribution of direct (CTb; a1 to n1) and indirect staining with PRV 152 (2 days post injection: a2 to n2; 3 days post injection a3 to n3). The last column illustrates the corresponding brain level according to the Franklin & Paxinos mouse brain atlas. Drawing result of a compilation of 4 animals for CTb, 4 for 2 days PRV and 4 for 3 days PRV.

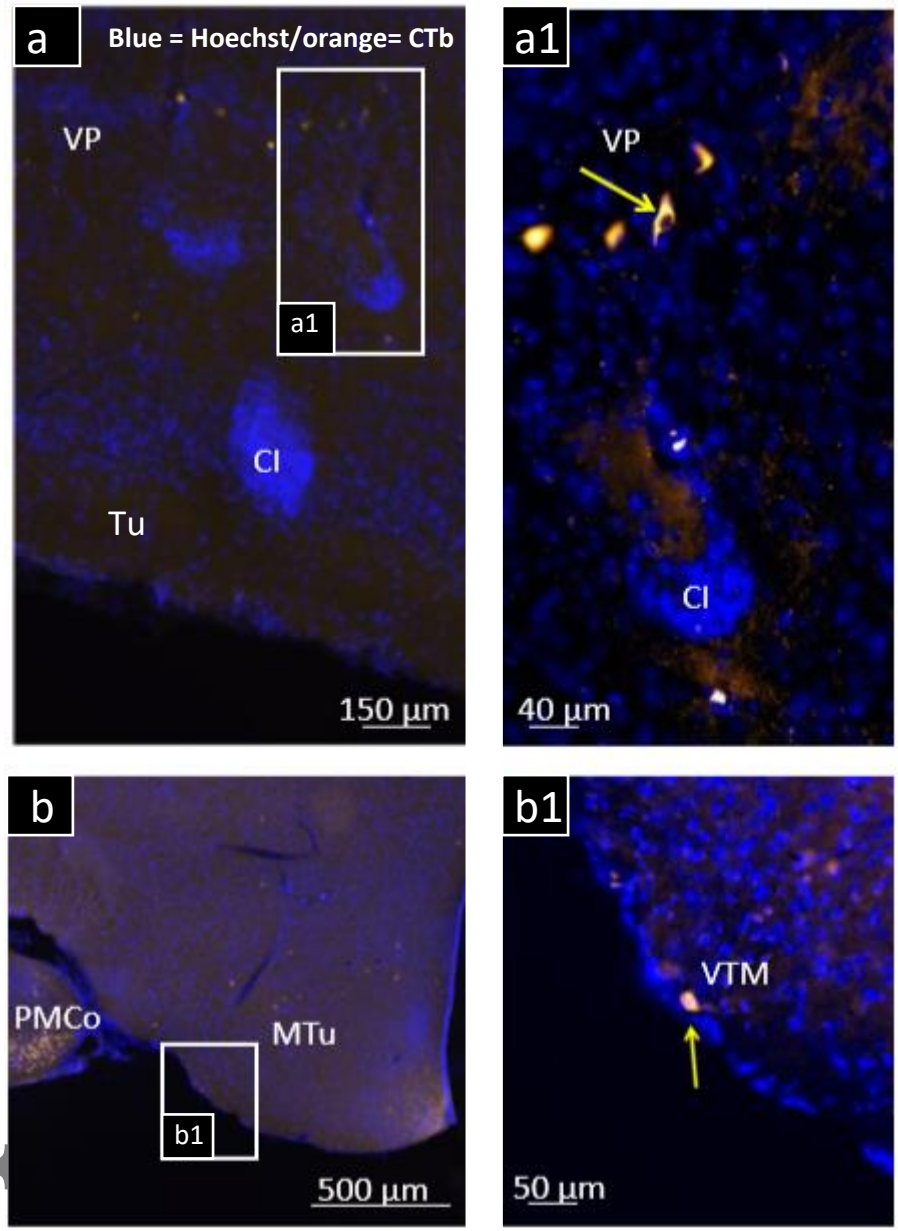

Figure 3. a-a1: Illustration at low and higher magnification of the CTb retrograde labeling in the ventral pallidum (VP) indicating a direct projection from the VP to the MOB. **b-b1**: Photomicrographs depicting at low and higher magnification a retrogradely CTb stained neuron in the ventral tubero mammillary nucleus (VTM). Blue staining is Hoechst nuclear staining to visualize nucleus.

Cl : Island of Calleja; **MTu:** medial mammillary nucleus; **PMCo:** posteromedial cortical nucleus of the amygdala ; **Tu** : Olfactory tubercle.

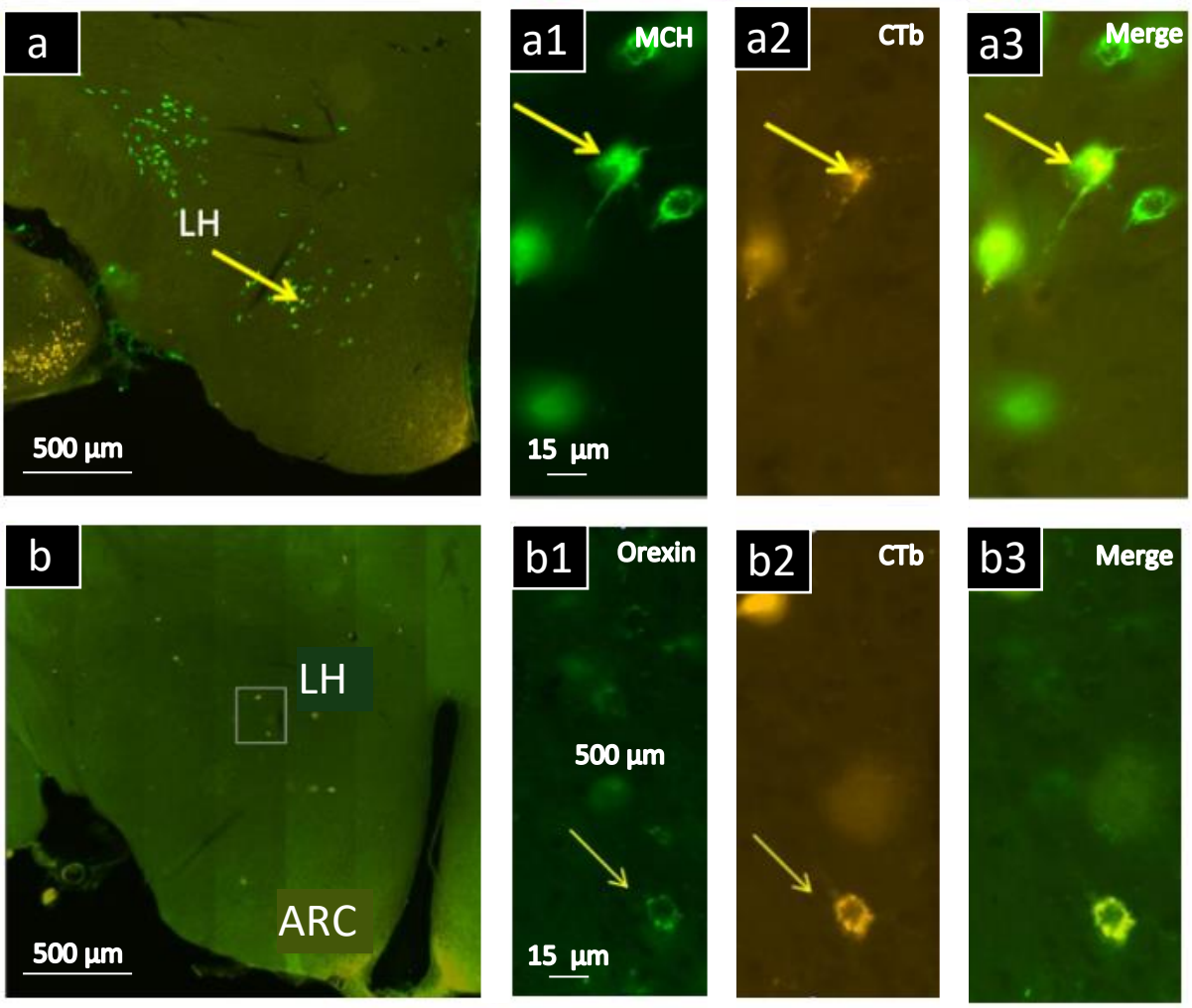

Figure 4. CTb injections in the main olfactory bulb (MOB) demonstrate a direct MCH and Orexin projection arising from the lateral hypothalamus (LH).

a: The MOB receives direct MCH projections from LH as demonstrated by colocalisation of CTb and MCH**. a1**: MCH immunostaining (green); **a2 :** CTb immunostaining (orange); a3**:** merge.

b: The MOB receives direct orexinergic projections from LH.**b1:** orexin immunostaining (green). **b2:** CTb immunostaining (orange). **b3:** merge.

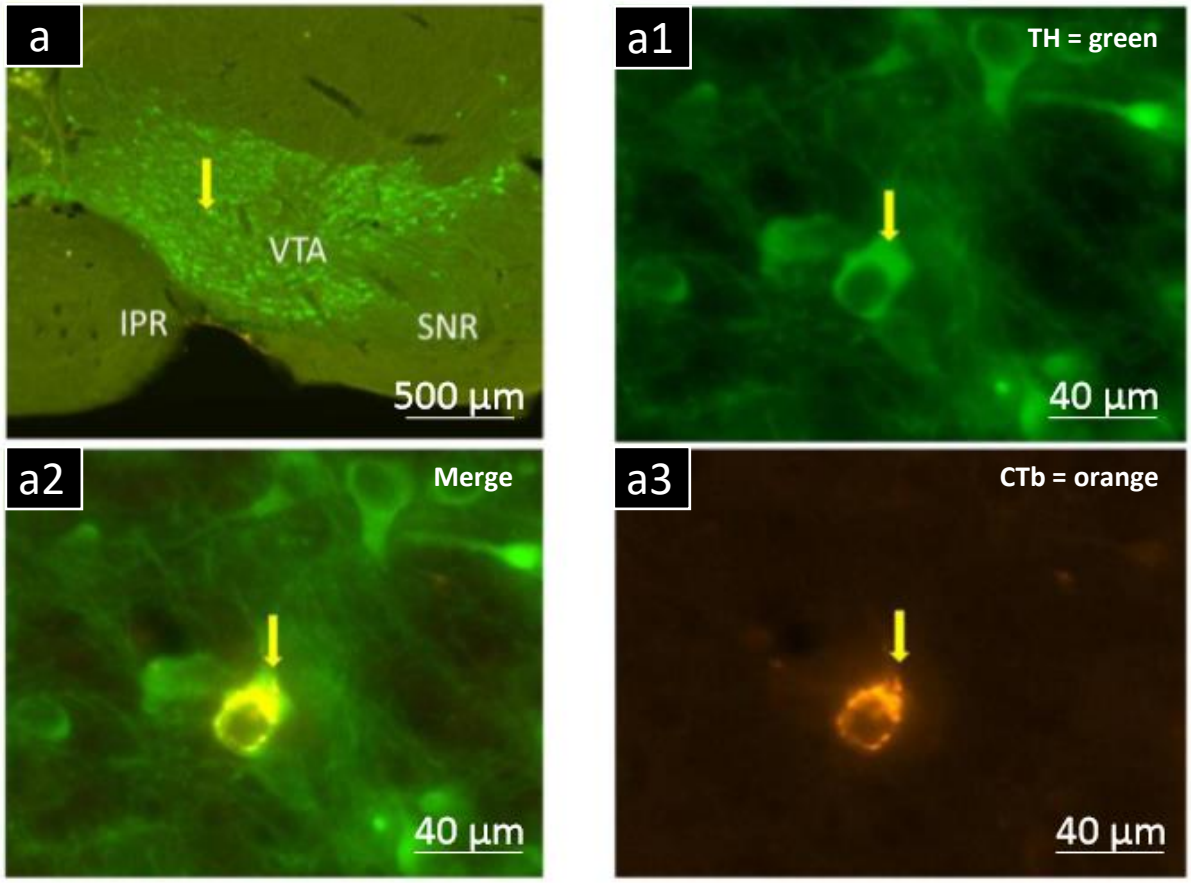

Figure 5. The ventral tegmental area (VTA) showed a low number of CTb retrogradely labeled neurons. Immunohistochemical staining against tyrosine-hydroxylase (TH) showed that the CTb stained cells were TH-positive, indicating a direct monoaminergic projection from the VTA to the main olfactory bulb. **a1**: TH immunostaining (green), **a2** : CTb immunostaining (orange), **a3**: merge.

IPR: interpeduncular nucleus; SNR: substantia nigra, reticular part.

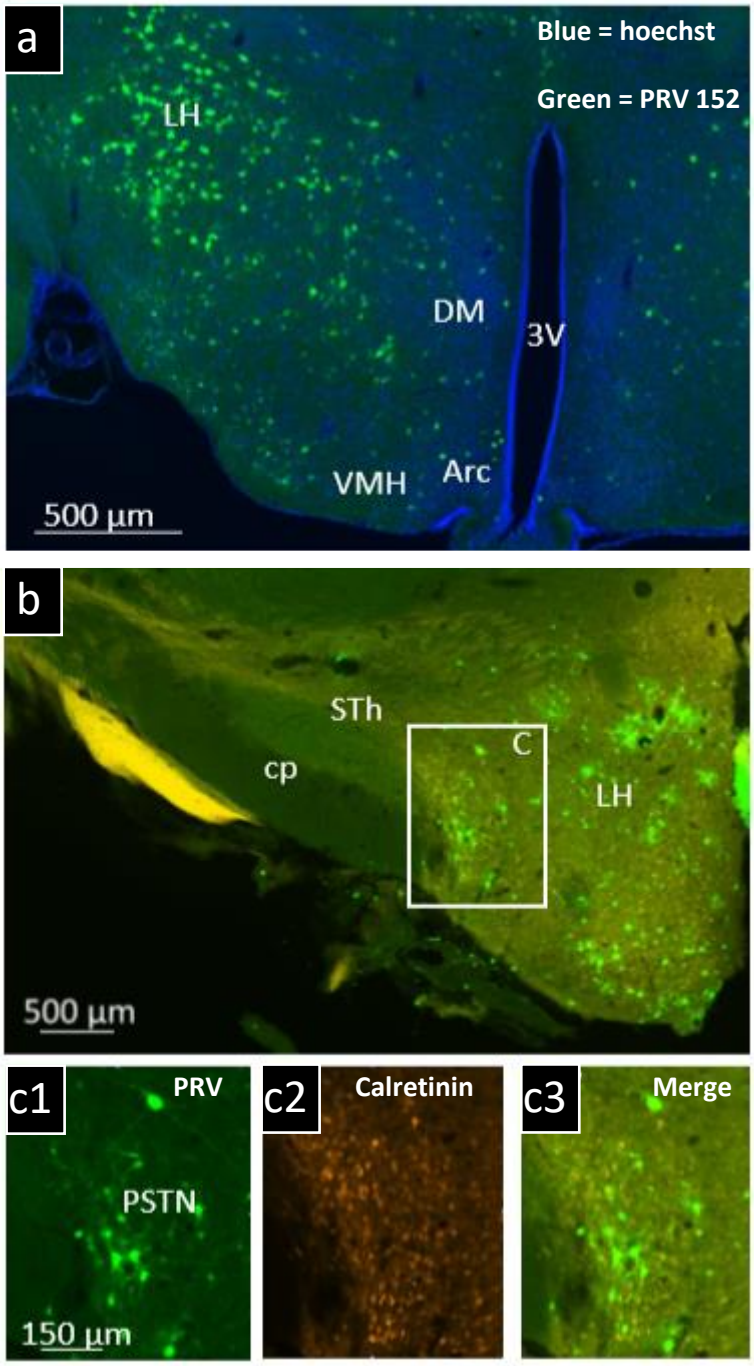

Figure 6. Illustration of the distribution of the neurons labeled by PRV 152 in the hypothalamus on the 3rd post-injection day. Indirect projections onto the MOB originate from several hypothalamic regions.
a: The lateral hypothalamus (LH) showed a substantial number of retrogradely labeled neurons. In contrast, a moderate labeling was observed in other hypothalamic areas such as the dorsomedial (DM), the ventromedial (VMH) and the arcuate (Arc) nuclei. Hoechst's blue staining allows visualization of nuclei.
b: Low magnification of the hypothalamus at the level of the parasubthalamus nucleus (PSTN) where a noticeable number of PRV 152 stained cells were observed. **c1**: High magnification of the PSTN: Some neurons were double-labeled for both PRV 152 and calretinin. PRV 152 immunostaining (green); **c2**: Calretinin immunostaining (orange), c**3:** merge.
Cp: cerebral peduncle; **STh:** subthalamus nucleus.

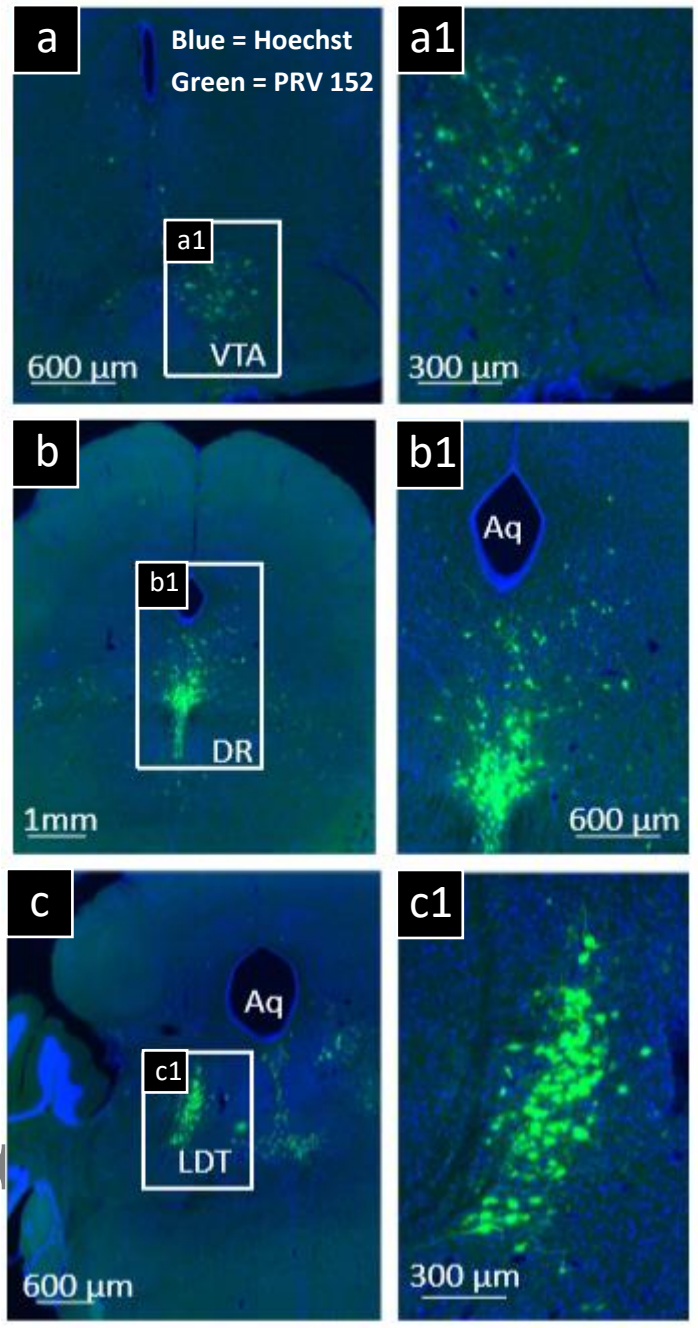

Figure 7. Low and high magnification of the indirect labeling observed following PRV 152 injection into the MOB showing projections from :

a-a1: the ventral tegmental area (VTA);

b-b1: the dorsal raphe (DR)

c-c1: the laterodorsal tegmental nucleus (LDT).

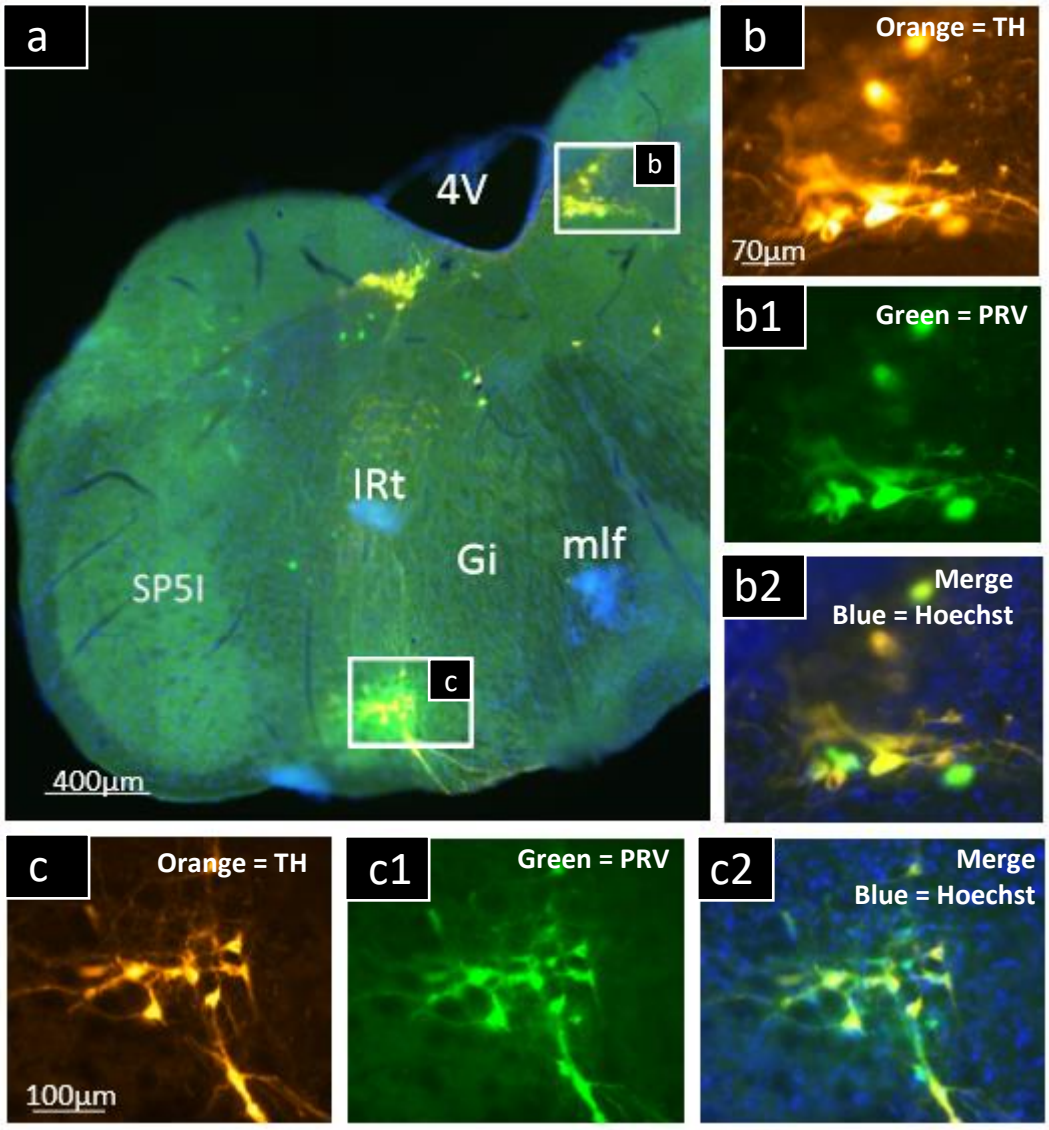

Figure 8. a: Low magnification microphotograph showing the distribution of PRV 152 labeled cells in the brainstem. **b:** The nucleus of the solitary tract (Sol) showed some retrogradely labeled cells that were also positive for TH (B: TH staining (orange); **b1**: PRV staining (green); b2: merge). The rostral ventrolateral medulla oblongata (RVLM) exhibited some retrogradely labeled cells that were also positive for TH (**C**:TH staining (orange); **c1**: PRV 152 staining (green); c2: merge).

Gi: gigantocellular reticular nucleus; **IRt**: intermediate reticular nucleus; **mlf:** medial longitudinal fasciculus; **SP5I:** Spinal trigeminal nucleus.

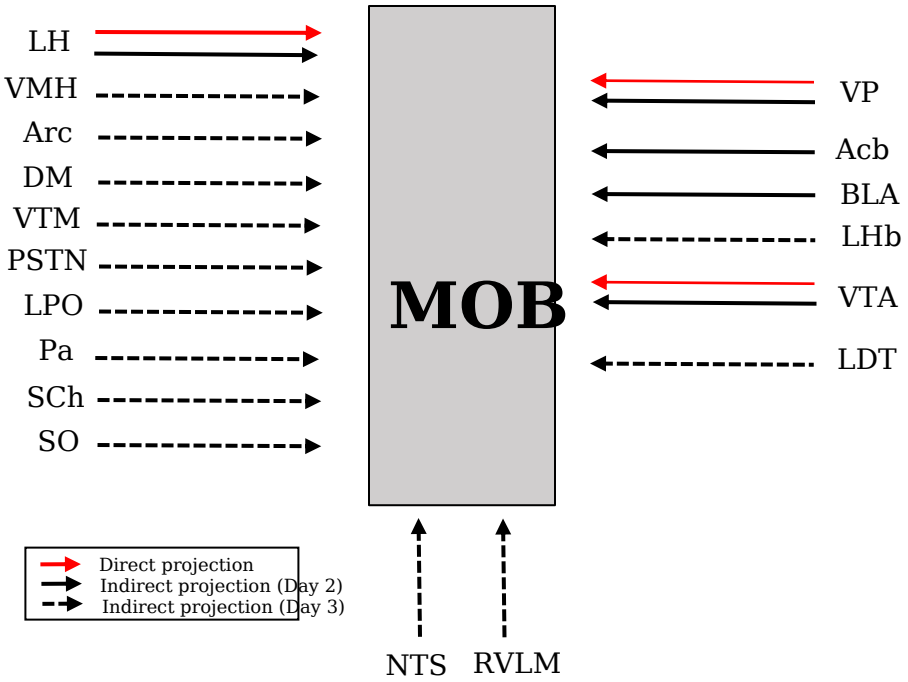

Figure 9: Schematic illustration of the monosynaptic and polysynaptic centrifugal projections onto the main olfactory bulb. The injections of either CTb or PRV in the MOB granular layer were used to retrogradely trace the direct (red arrows: CTb labeling) and indirect (filled black arrow: PRV labeling 2 days-post injection; dot black arrows: PRV labeling 3 days-post injection) centrifugal projections. Analysis of the distribution of the retrogradely labeled neurons focused on feeding- related areas. In the hypothalamus, the LH sends both direct and indirect projections. All the other hypothalamic nuclei showed only polysynaptic centrifugal connections with the MOB. Among regions involved in the reward circuitry, the VTA and VP send both direct and indirect projections. The present tracing study was descriptive. Nevertheless, despite the lack of quantitative analysis, we used a thiner arrow to indicate that a low number of neurons were CTb stained. The MOB is the target of indirect projections arising from the brainstem (NTS and RVLM). See table for abbreviations.